Economic Geology
Vol. 76, 1981, pp. 580–609

Silver Mineralization in the Rochester District, Pershing County, Nevada

PETER G. VIKRE

ASARCO Incorporated, Southwestern Exploration Division, Box 5747, Tucson, Arizona 85703

Abstract

The Rochester district encompasses a number of precious metal vein deposits which produced $7 million in silver and gold from 1912 to 1928. The largest deposits were mined on Nenzel Hill where over 100 million tons of low-grade silver-gold mineralization have recently been defined. The veins and low-grade mineralization occur in rhyolites of the Permian-Triassic Koipato Group. The Koipato Group includes mafic to siliceous volcanic and intrusive rocks scattered throughout north central Nevada. Overlying Mesozoic sedimentary rocks, once more than 11,000 ft thick in the vicinity of Rochester, have been severely eroded since the inception of Tertiary basin and range tectonism. Koipato rhyolites were hydrothermally altered on a regional scale to quartz-sericite-pyrite as a result of both the emplacement of comagmatic Koipato intrusives and Late Cretaceous stocks. Precious metal mineralization at Rochester probably accompanied the Late Cretaceous event.

The major veins of Nenzel Hill comprise two mineral assemblages which fill and replace faults and strongly fractured rhyolite. Stage 1 veins consist of quartz, K-feldspar, and base and precious metal sulfides. They occur as open space filling and are confined to deeper portions of the Nenzel Hill mineralized zone. Stage 2 veins consist of a similar assemblage but cut stage 1 veins and display strong vertical zoning. With increasing elevation, stage 2 silver minerals are more abundant, Ag/Au increases, and sericite becomes prevalent. In stage 2 veins the FeS content of sphalerite varies from >11 to <1 mole percent over 800 vertical feet, with iron-poor sphalerites occurring nearer to the present surface. The stage 2 assemblage of quartz, sericite, sulfides, and sulfosalts is most common on intermediate and near-surface levels in Nenzel Hill. Low-grade mineralization consists largely of oxidized (80%) and unoxidized (15%) stage 2 assemblages which fill thin, randomly oriented, closely spaced fractures between major veins. Some precious metal grade (5%) is derived from wall-rock pyrite. The low-grade deposit is best developed within several hundred feet of the present surface but appears not to be significantly enriched.

Fluid inclusions, oxygen isotopes, mineral compositions, and stabilities and stratigraphic reconstruction indicate that Nenzel Hill mineralization formed at about 300°C and 1 kb. The major components of ore fluid were water, carbon dioxide, and solute approximated by $(Na_{0.843}Ca_{0.075}K_{0.006}Mg_{2.2 \times 10^{-4}})Cl$. Vein sulfides, silicate alteration phases, and sphalerite compositions indicate that f_{S_2} and f_{O_2} of ore fluid in major conduits progressively increased with elevation. The marked correlation of these changes in fluid composition with silver grade suggests that precious metal distribution was governed by hypogene processes. Buffering of the ore solution by a K-feldspar + sericite + quartz wall-rock assemblage permitted dispersion of metal values for great distances from main channel ways, forming a large tonnage of low-grade mineralization.

Introduction

THE Rochester district is in the Humboldt Range about 25 miles northeast of Lovelock, Nevada (Fig. 1). Within the district precious metals valued at $7 million were mined mainly from vein deposits in Nenzel Hill during the period 1912 to 1928. Production was 720,000 tons, averaging 12 ounces of silver and 0.10 ounces of gold per ton (Vanderburg, 1936; Couch and Carpenter, 1943; Johnson, 1977). The veins occur in Permian-Triassic rhyolites of the Koipato Group. Recent drilling on Nenzel Hill by ASARCO Incorporated has defined more than 100 million tons of mineralized rhyolite containing 1 to 2 ounces of silver and small amounts of gold per ton.

Early descriptions of the veins are given by Schrader (1914) and Knopf (1924). Subsequent geological work in the central part of the Humboldt Range has been concerned with petrology and stratigraphy of Mesozoic rocks (Jenney, 1935; Cameron, 1939; Silberling and Wallace, 1967; Wallace et al., 1969a, 1969b; Silberling and Wallace, 1969). Current emphasis on exploration and surface mining of precious metal deposits prompted this study of the Rochester district.

Geologic Setting

The Humboldt Range is an elongate horst bounded by high angle, normal faults of considerable displacement. Exposed in the range are late Paleozoic and

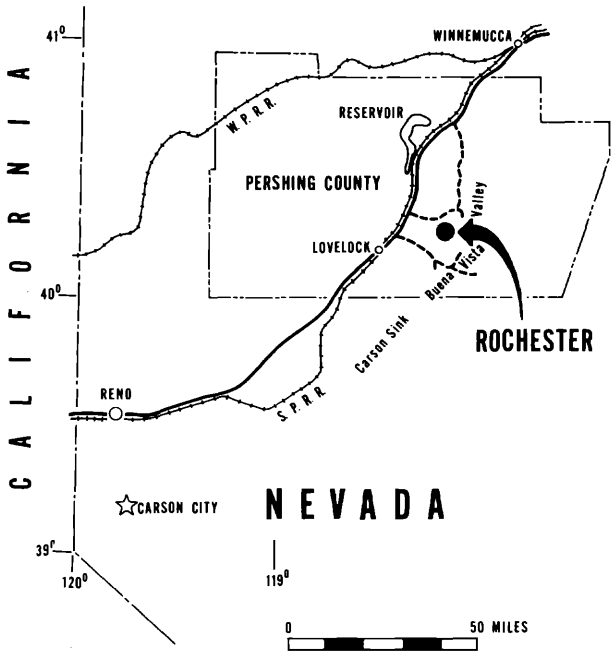

FIG. 1. Index map of Pershing County, Nevada, showing the location of the Rochester district.

Mesozoic extrusive, intrusive, and sedimentary rocks in which occur a variety of ore deposits (Ransome, 1909; Kerr and Jenny, 1935; Kerr, 1938, 1940; Cameron, 1939; Campbell, 1939; Bailey and Phoenix, 1944; Vitaliano, 1944; Vikre, 1977). Volcanic, sedimentary, and intrusive rocks of the Permian-Triassic Koipato Group are distributed throughout the range and underlie the Rochester district (Figs. 2 and 3). The predominantly rhyolitic Koipato volcanism followed the collapse of a western marginal basin and eastward movement of basinal facies along the Golconda thrust (Sonoma orogeny). Chemical compositions and stratigraphic relations of the Koipato members suggest that the volcanic rocks may be late differentiates of subducted oceanic and melted continental crust (Silberling, 1973).

A sudden change in crustal stability was marked by the gradual subsidence of the western continental margin. Erosion of part of the Koipato Group was followed by Triassic deposition of a thick sequence of chemical and clastic sediments including the Star Peak Group (Silberling and Wallace, 1969) and Grass Valley Formation. Koipato rhyolites in the Humboldt Range may have been covered by 12,000 ft of marine sedimentary rocks by the mid-Mesozoic. Plutonism and regional deformation (Willden, 1961; Wallace and Silberling, 1965) sponsored uplift, faulting, and folding of the entire section during the late Mesozoic.

Following extensive early Tertiary erosion, Miocene gravels and a bimodal assemblage of rhyolite and basalt were deposited in the vicinity of Nenzel Hill. Post-Miocene erosion removed nearly all Tertiary rocks, much of the Mesozoic sequence, and some precious metal mineralization. Triassic rocks which overlie Koipato rhyolites along both flanks of the Humboldt Range partly define a broad, north-trending antiform centered on the Rochester district (Fig. 3).

Koipato Group

In the Rochester district, the Koipato Group includes the Limerick, Rochester, and Weaver Formations, in order of decreasing age. The Limerick Formation consists of intermediate to mafic intrusive, eruptive, and volcaniclastic rocks which are overlain by two rhyolites of slightly differing age. The older rhyolite, the Rochester Formation, is predominantly tuff, with subordinate flow and clastic rocks. It is overlain unconformably by rhyolitic flows, ash-flow tuffs, and clastic strata of the Weaver Formation. The Limerick and Rochester Formations are intruded by fine- to medium-grained granite, interpreted to be the parent magma of the Rochester eruptives. Recurrent magmatism resulting from the emplacement of granite stocks was accompanied by eruption of Weaver rhyolite from linear and oblate vents. Melt remaining in the vents solidified to rhyolite porphyry. Fluvial deposits between the two eruptive rhyolites and granite fragments with diagnostic micrographic texture in Weaver ash flows attest to a depositional hiatus during Koipato rhyolitic volcanism. Chemical compositions of all Koipato siliceous rocks are remarkably similar, suggesting a common source. Fossils indicate an Early Triassic age for upper Koipato strata (Silberling, 1973). Rocks of the Koipato Group fit an Rb-Sr isochron of 235 m.y. (R. C. Speed and R. Kistler, 1975, pers. commun.) and have a fission track age of 225 ± 30 m.y. (McKee and Burke, 1972). In the Rochester district Koipato rocks are unconformably overlain by Early Triassic limestones and dolostones of the Star Peak Group.

Contact hydrothermal alteration

Two plutonic events, widely spaced in time, caused bulk chemical changes and recrystallization in Koipato rocks throughout the Humboldt Range. The first event involved intrusion of Permian-Triassic granite. A second event occurred about 70 to 80 m.y. ago (Silberman et al., 1973; Vikre, 1977), with the emplacement of stocks related to the Sierra Nevada batholith (Smith et al., 1971). Ore deposition in the Rochester district probably coincided with the latter event. Cretaceous intrusive rocks vary in composition from quartz monzonite to granodiorite. They are mainly exposed north of the Rochester district and are represented near Rochester by several breccia dikes and small plugs of granodiorite. High magnetic

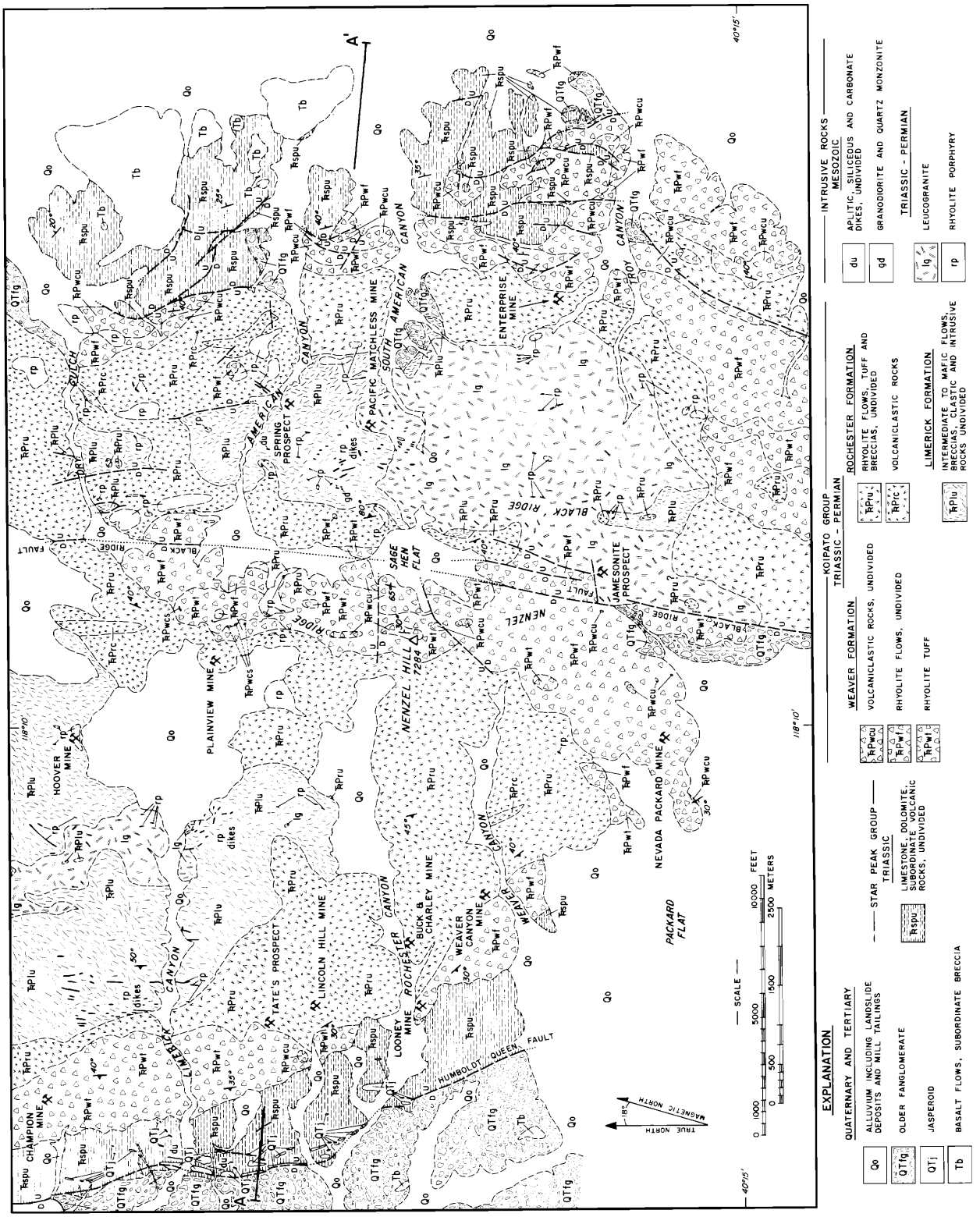

FIG. 2. Geologic map of the Rochester district.

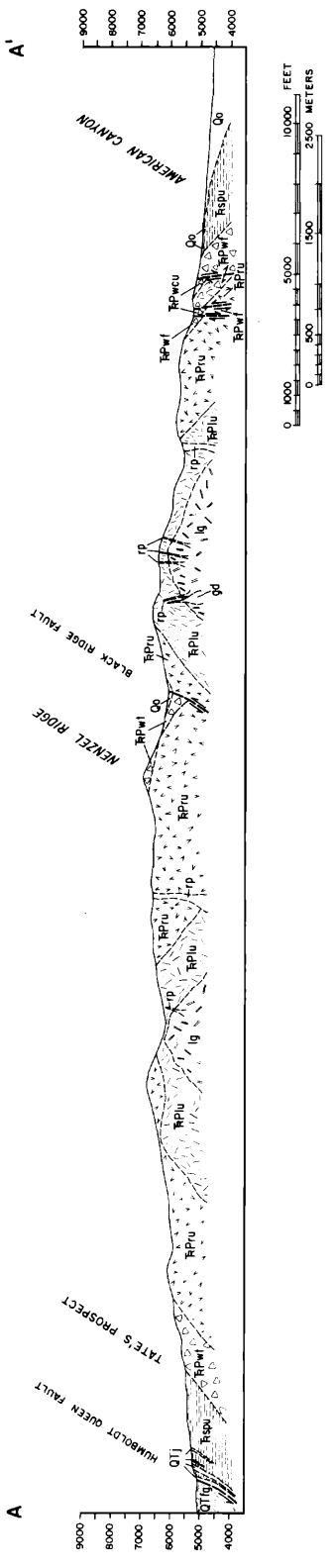

FIG. 3. Geologic section of the Rochester district. For explanation see Figure 2.

intensities (Fig. 4) are assumed to indicate the shallow level position of concealed, larger intrusions. Hydrothermal alteration and warping of Koipato rocks are associated with both episodes of intrusion. The superimposed effects of Koipato-related and Late Cretaceous alteration are difficult to separate because of the widespread and overlapping distribution of similar hydrothermal mineral assemblages.

In the Rochester district contact hydrothermal alteration caused by emplacement of the Permian-Triassic granite produced quartz, sericite, pyrite, and minor amounts of albite and calcite in large volumes of Rochester rhyolite. Contemporaneous epidote-albite-calcite-chlorite alteration occurs in underlying mafic volcanic rocks of the Limerick Formation.

The distribution and intensity of contact hydrothermal alteration in the Rochester district are somewhat asymmetrical (Fig. 4) but directly related to the outcrop or the magnetically inferred locations of intrusive rocks. Quartz, sericite, and pyrite comprise up to 90 percent of Rochester rhyolite in the vicinity of Koipato granite. Nearly all matrix, phenocrystic, and lithic feldspars have been altered to quartz, sericite, and pyrite. Pyrite is noticeably more abundant in sericitized phenocrysts and rock clasts, and is apparently coeval with sericite and quartz. Adjacent to intrusive rocks, Rochester rhyolite is completely recrystallized to quartz-sericite ± pyrite schist in which all primary texture is obliterated. On the north slope of Limerick Canyon (Figs. 2 and 4), foliated quartz-sericite-pyrite-altered rhyolite, greatly thinned by postgranite erosion, is disconformably overlain by relatively unaltered ash-flow tuffs of the Weaver Formation. Weaver ash flows thus postdate contact alteration by Koipato granite and clearly document the Permian-Triassic age of this alteration event.

Tourmaline and fluorine-bearing minerals, including phlogopite, apatite, and taeniolite (a potassium-magnesium mica), are restricted to veins, vugs, and local strata in lower Koipato eruptive rocks. Tourmaline is very abundant in fractures in granite cupolas. These minerals are rare to absent in Weaver rocks and are therefore considered to be associated with Permian-Triassic magmatism. Alteration of Weaver rocks, unrelated to resurgent Koipato magmatism, occurred mainly in the Late Cretaceous. Quartz, sericite, and pyrite are regionally distributed in the Weaver Formation, but far more unaltered phenocrystic and matrix feldspar remains than in Rochester rocks. In a roughly linear but discontinuous zone along the west flank of the Humboldt Range, both Koipato Group rhyolites are altered to quartz-sericite schist with accessory andalusite, dumortierite, and cordierite (Fig. 4). Transection of formational boundaries by these minerals and proximity to the large mass of Late Cretaceous intrusive rock at Rocky

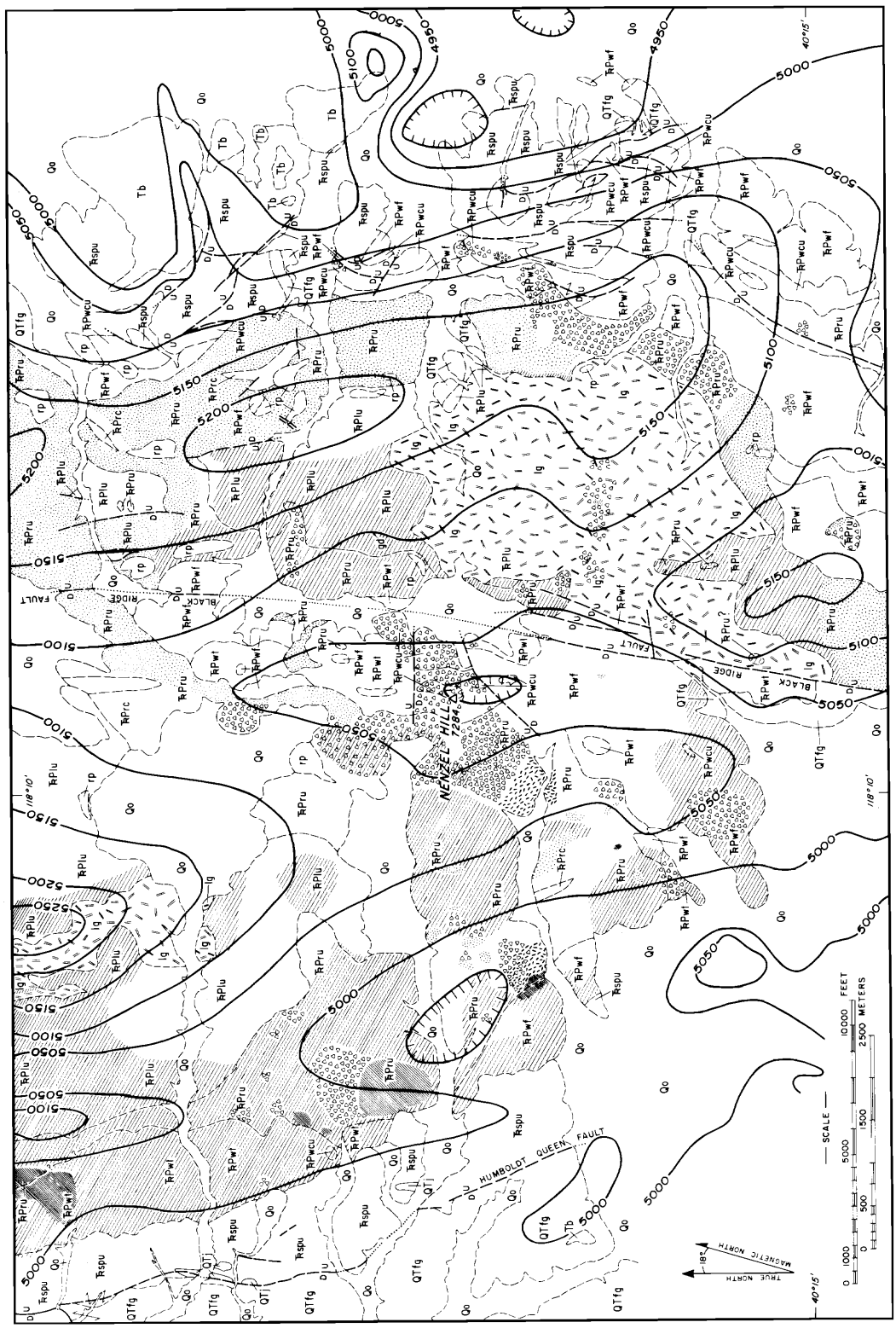

FIG. 4. Distribution of hydrothermal assemblages and intrusive rocks in the Rochester district. Intrusive lithology is from Figure 2 and the area of the figure is the same as Figure 2.

Canyon (Wallace et al., 1969b) suggest that the quartz - sericite - dumortierite - andalusite - cordierite schists formed during Late Cretaceous plutonism. Thorough sulfidation of iron phases in Koipato intrusions indicates that Cretaceous stocks containing accessory magnetite may cause most of the magnetic peaks in Figure 4.

The overprint of Late Cretaceous alteration on Koipato-related alteration may also be represented by conjugate foliations in Rochester and Weaver rocks on the western side of the range. Attitudes suggest that one planar orientation is related to the regional antiformal trend (N to N 35° W strike, 30° to 40° dip; Fig. 2) of pervasive, Late Cretaceous-induced schistosity along the west flank of the range while a second foliation (N 15° E to N 35° W, 10° to 75° W) probably formed concurrently with Permian-Triassic alteration of lower Koipato eruptives. Variation in attitude of Koipato-age foliations reflects the irregular leucogranite surface indicated by outcrop distribution and recrystallized Rochester eruptives (Fig. 4).

Two distinct alteration epochs in the Humboldt Range are more easily recognized north of the Rochester district where intrusive rocks of differing age are not as closely juxtaposed. Detailed microscopy (Jenney, 1935; Kerr and Jenney, 1935; Cameron, 1939) and chemical analyses (Tatlock, 1961) define earlier albitic and biotitic alteration of Koipato rocks, partly destroyed by a later quartz-sericite-pyrite assemblage.

Variable amounts of accessory pyrite and hematite occur in Koipato rocks throughout the Rochester district (Fig. 4). Hematite microlites reside only in matrices of less altered eruptives and may reflect a magmatic component. Pyrite, which never occurs with hematite, appears to have crystallized with sericite and quartz. Pyrite, sericite, and quartz replaced matrices, phenocrysts, and clasts during sulfidation of iron oxide. Often pyrite is intergrown with titanium oxide (probably anatase) in composite grains of cubic habit. TiO_2 may be residual from titanium-bearing magnetite or ilmenite. The presence of pyrite in Koipato rhyolites at great distances from epigenetic deposits and intrusive rocks, and its relation to iron and titanium oxides, suggests that it initially crystallized soon after eruption of the volcanic rocks and is partly independent of precious metal vein mineralization. Additional pyrite undoubtedly formed in Koipato rocks during Late Cretaceous plutonism in the Humboldt Range, particularly in the vicinity of vein deposits. Pyrite throughout the Rochester district contains significant amounts of silver and gold (Table 1). Less altered Koipato rhyolite elsewhere in north central Nevada may contain several percent iron oxide, probably as a primary mineral. These dark-colored rhyolites do not contain detectable precious metals. Thus, introduction of trace precious metal to the Koipato pile in the Rochester district apparently accompanied sulfidation of iron oxides. The exact age of sulfidation is unknown and the widespread introduction of silver, gold, and sulfur could have occurred several times.

Temperature limits may be placed on contact hydrothermal alteration assemblages in the Rochester district. The ubiquitous quartz + sericite + pyrite assemblage in altered Koipato rhyolites indicates that most alteration lies within the quartz + muscovite stability field, or near the quartz + muscovite + K-feldspar univariant curve of Montoya and Hemley (1975). The presence of muscovite limits temperatures during alteration to less than about 550°C, assuming $[SiO_2] = 1$ and $P_{volatiles} = P_{total}$. Nowhere in the Rochester district do K-feldspar and andalusite coexist, which would permit temperatures in excess of 550°C. Pyrophyllite and kaolinite are absent from regional alteration assemblages. Unless $[K^+]/[H^+]$ in pore fluids increased uniformly on a district-wide scale or $P_{total} > P_{volatiles}$, temperatures during contact hydrothermal alteration were consistently above about 300°C (see Montoya and Hemley, 1975, fig. 1). Quartz-muscovite temperatures, based on oxygen isotope fractionation, for the quartz + sericite + andalusite + dumortierite assemblage in altered Koipato rhyolites along the western flank of the range, and from quartz + sericite + precious metal veins in rhyolite adjacent to these aluminous strata, indicate that maximum temperatures during contact hydrothermal alteration and mineralization were on the order of 500°C (B. E. Taylor, pers. commun.).

Vein-Related Alteration

Most vein deposits in the Rochester district, including those in siliceous Koipato rocks, are enveloped by a quartz-sericite-pyrite alteration assemblage. Similar physical and chemical conditions, and probably contemporaneity of pervasive contact and vein hydrothermal alteration in the Late Cretaceous, have produced mineral assemblages that are common to each variety of alteration. Locally the distribution of sericite and pyrite that crystallized in wall rock during vein filling is largely inseparable from sericite and pyrite produced by regional contact hydrothermal alteration.

Silicification is proximally related to most epigenetic mineralization but also occurs independently of metal values and quartz veining. The term silicification is used here in its broadest sense to include silica locally added to or regionally redistributed within Koipato rhyolites, epigenetic quartz introduced along fractures, the formation of groundmass silica from devitrification of glass, and the development of SiO_2 from feldspar alteration. The majority

TABLE 1. Silver and Gold Concentrations (ppm) in Disseminated, Optically Homogeneous Pyrite and Whole-Rock Samples Visually Free of Epigenetic Veins

Location, host rock; sample number	Pyrite separate		Whole rock	
	Au	Ag	Au	Ag
Pitt level, Nenzel Hill, Weaver ash-flow tuff; P-17	1.0	140	ND	2.0
Pitt level, Nenzel Hill, Weaver ash-flow tuff; P-15	<0.02	330	<0.05	2.2
Pitt level, Nenzel Hill, Rochester tuff; ⑬ 207′	1.3	68	ND	2.0
Pitt level, Nenzel Hill, Rochester tuff; ⑬ 295′	<0.02	83	0.16	17.0
Freidman level, Nenzel Hill, Rochester flow; F-7	5.8	40	0.10	2.0
Nevada Packard open pit, Weaver flow; NP-HB	0.5	315	ND	4.0
Limerick Canyon mine, Limerick greenstone; LCM-1	0.10	4	<0.05	1.0
Rolands Canyon, Weaver flow; RC-1	<0.02	34	<0.05	1.0
Pacific Matchless mine, granite; PM-2	0.10	10	<0.05	2.0
Nenzel Ridge prospect, Weaver ash-flow tuff; NR-1	<0.02	410	<0.05	21.0
Buck and Charley ridge, Rochester flow; BC-2	1.2	60	0.10	10.0

Analyses include Koipato wall rocks from vein deposits and Koipato rocks at considerable distances from known mineralization. Pyrite separates were obtained using density contrast and magnetic methods. All analyses are by atomic absorption (ASARCO Geochemical Lab, Salt Lake City, Utah; Skyline Labs, Inc., Tucson, Arizona). ND means none detected.

of low-grade mineralization at Nenzel Hill occurs in topographically prominent Weaver ash-flow tuffs and clastic rocks. The originally siliceous composition of the Weaver flows and tuffs and silicification of the rhyolite by quartz veining are evidenced by the erosional resistance of Nenzel Ridge on the Humboldt Range divide.

Examination of numerous thin sections of wall rock adjacent to and many feet from both narrow mineralized veins and major veins (arbitrarily those more than 1 ft thick) reveals only poorly definable mineralogical changes in Nenzel Hill rhyolites. Groundmass both near and far from veins is largely recrystallized into a quartz + sericite + K-feldspar + pyrite mosaic. Overall, the groundmass is microcrystalline, suggesting little addition of components. Feldspar staining with cobaltinitrate indicates that much of the matrix texture represents either devitrification or K-feldspar alteration to sericite and quartz, rather than introduced silica related to vein-forming hydrothermal fluids.

Distinctly coarser grained quartz locally forms inequigranular and irregular aggregates throughout the tuffs and flows regardless of proximity to the veins, but near the closely spaced veins on Nenzel Hill coarse-grained quartz in matrices is more abundant. It comprises up to 10 volume percent of the rhyolite. The increase in silica as major veins are approached is sudden, irregular, or subtle. Strong vein-related silicification usually does not extend more than a few feet into the wall rock but often coalesces with silicification adjacent to other veins. Some vein breccia fragments are marginally replaced by a thin seam of slightly clearer and coarser grained quartz. The borders of others merge with equigranular, microcrystalline silica.

Some mineralized veins have sharp borders with enclosing wall rock, but all degrees of marginal replacement by silica are evident. Fine-grained quartz-sericite intergrowths may completely replace tuffaceous groundmass for several tenths of inches from quartz-sulfide stringers and render vein contacts indistinct. Coarser grained xenomorphic quartz aggregates display, in part, patchy undulose extinction, possibly indicative of coalescence of smaller grains during partial recrystallization. Such thoroughly silicified rhyolite is extremely hard and usually preserves unoxidized sulfides in the underground workings. Less silicified tuff, even though unfractured, may lack unweathered sulfides and sulfosalts.

Orthoclase and microcline phenocrysts in Weaver rhyolite adjacent to veins may be well preserved or only partly sericitized, and unaltered K-feldspar occurs at the contacts of quartz veins. Orthoclase in breccia fragments within major veins is usually recrystallized and/or sericitized. Feldspars of rock fragments in the ash flows in contact with veins are generally sericitized and pyritized. The distinct difference in alteration intensity between feldspars in clasts and feldspar phenocrysts in ash flows suggests that some clast alteration may have occurred prior to or concomitantly with eruption of the tuffs.

Chemical changes in Koipato rhyolites generally support petrographic observations. The composition of altered Rochester eruptives in Nenzel Hill (analyses C, D, and E, Table 2) differs only slightly from that of unmineralized rhyolite (analyses A and B, Table 2). The loss of sodium, effected by complete sericitization of plagioclase, and an increase in iron, largely as pyrite, are the most distinctive mass changes. Weaver ash-flow tuffs in Nenzel Hill show similar trends for Na_2O and Fe but also display marked losses

TABLE 2. Partial Chemical Analyses and Selected Trace Elements of Eruptive Rocks in the Rochester (A–E) and Weaver (F–I) Formations and Veins (J–L) in Nenzel Hill

	Rochester rhyolite					Weaver rhyolite				Veins in Nenzel Hill		
Sample no.	A	B	C	D	E	F	G	H	I	J	K	L
Field no.	79119	79120	RD79-3	RD79-4	RD79-9	RD79-5	57W387	RD79-2	RD79-1	RD79-8	RD79-10	RD79-11
Weight percent												
SiO_2	78.0	77.3	78.7	73.6	74.9	72.2	75.00	83.9	82.5	85.7	93.0	94.2
Al_2O_3	11.1	11.1	10.6	13.4	12.1	19.1	13.40	8.7	10.2	5.3	2.6	0.90
Fe_2O_3	0.77	0.77	1.8	1.2	1.4	0.21	0.30	1.2	0.57	3.7	2.1	1.8
FeO	0.13	0.13	0.01	0.02	0.02	0.02	0.50	0.01	0.08	0.02	0.13	0.06
MgO	0.17	0.11	0.10	0.22	0.16	0.04	0.13	0.34	0.42	0.32	0.15	0.06
CaO	0.13	0.13	0.04	0.05	0.05	0.06	0.08	0.05	0.06	0.03	0.06	0.06
Na_2O	0.50	1.3	0.19	0.23	0.20	0.67	0.30	0.16	0.15	0.03	0.01	0.01
K_2O	8.4	8.2	8.0	9.0	9.0	4.9	9.60	5.8	6.3	3.1	1.2	0.47
TiO_2	0.08[1]	0.12[1]	0.33[1]	0.25[1]	0.33[1]	0.25[1]	0.07	0.17[1]	0.17[1]	0.08[1]	tr[1]	0.003
BaO	0.08[1]	0.08[1]	0.34[1]	0.34[1]	0.11[1]	tr[1]	—	0.22[1]	0.11[1]	tr[1]	tr[1]	0.001
H_2O^+	—	—	—	—	—	—	0.55	—	—	—	—	—
S	0.05	0.05	1.4	0.05	1.1	0.01	—	0.86	0.05	2.8	0.89	0.54
Total	99.36	99.04	101.50	98.29	99.37	97.39	99.93	101.40	100.56	101.06	100.14	98.09
S.G.	2.59	2.59	2.64	2.59	2.65	2.72	2.60[2]	2.62	2.56	2.66	2.67	2.65
Au ppm	0.02	0.02	0.16	0.02	0.02	0.02	—	0.02	0.02	0.54	0.52	3.5
Ag ppm	1.0	0.02	17.0	1.8	1.8	0.8	—	2.2	1.0	34.0	280.0	350.0
As ppm	20.0	10.0	130.0	80.0	180.0	10.0	—	140.0	70.0	510.0	390.0	680.0
Sb ppm	1.0	1.0	70.0	20.0	4.0	10.0	—	11.0	9.0	27.0	200.0	930.0
Hg ppm	0.02	0.04	0.25	0.22	0.08	0.03	—	0.14	0.05	0.04	3.7	8.6

A, rhyolite flow, near Fencemaker Pass, Pershing County, Nevada
B, similar to A
C, rhyolite flow, Pitt level, Nenzel Hill, Pershing County, Nevada; altered and mineralized
D, similar to C
E, similar to C
F, rhyolite flow, Nenzel Ridge, 0.5 miles south of Nenzel Hill
G, rhyolite ash-flow tuff, Limerick Canyon (R. E. Wallace, 1975, pers. commun.)
H, rhyolite ash-flow tuff, Pitt level, Nenzel Hill, 250 ft from Stokely vein; altered and mineralized
I, rhyolite ash-flow tuff, west slope, Nenzel Hill, 150 ft from West vein; altered and mineralized
J, Caroline vein, Pitt level, Nenzel Hill, containing abundant wall-rock fragments
K, Stokely vein, Pitt level, Nenzel Hill, containing sparse wall-rock fragments
L, West vein, ~500 level, Nenzel Hill, consisting of quartz, sulfides, and minor sericite
[1] Estimated from spectrographic analysis
[2] Assumed
Tr = trace; < = lower than limit of detection; — = not analyzed; iron from pyrite is reported as Fe_2O_3; S.G. = specific gravity
All analyses except G are by Skyline Labs, Inc. (Tucson, Arizona)

of Al_2O_3 and K_2O with major vein development. SiO_2 increases as veins are approached and replacement of wall rock and fault gouge becomes complete (analyses G through L). Gold, silver, antimony, arsenic, mercury, and sulfur concentrations in mineralized Weaver rhyolite increase sharply with degree of alteration.

Silver Mineralization at Nenzel Hill

Precious metal mineralization at Nenzel Hill differs from other deposits in the Humboldt Range in terms of lithologic setting, sulfide-gangue textures, and mineralogy. It is economically separable into moderately rich vein deposits, largely mined out by 1928, and low-grade mineralization that is of current interest. The two types of mineralization are genetically related but somewhat structurally distinct.

Vein distribution and structure

The sites of precious metal vein mineralization throughout the Rochester district are fault zones which probably resulted from Late Cretaceous plutonism and deformation. In the vicinity of Nenzel Hill, faults hosting silver mineralization developed in the crest and flanks of an asymmetrical fold. Intercalated clastic lenses in Weaver ash-flow tuffs define this structure, a limb of which forms Nenzel Hill (Fig. 5). The strike of the fold axis is northeast and the axial plane dips about 45° west, largely because of tilting of the Humboldt Range in the Tertiary. The fold is truncated by the Black Ridge fault which traverses Sage Hen flat and by several east-west faults of considerable displacement (Figs. 2 and 5).

Distribution of major quartz-sulfide-sulfosalt veins in Nenzel Hill is shown in Figure 5. The veins are

both laterally and vertically discontinuous. Individual segments may be only a few feet long, but major veins consist of numerous aligned and semiparallel segments that are several thousand feet in composite length. The vein system has a curvilinear projection which strikes north to N 30° E. The thickest veins crop out near the top of Nenzel Hill (el. 7,284) and to the north along Nenzel Ridge. Narrower veins, generally of lower grade, occur on the east and west flanks of Nenzel Hill. They are approximately parallel to those at the top but are more widely spaced. The narrower veins are poorly exposed and many were discovered by underground mining.

Veins thin considerably or terminate with depth. On the Friedman level, 850 ft below the top of Nenzel Hill, the East and West veins rarely exceed 2 ft in width. Unmined East vein segments at the top of Nenzel Hill are more than 10 ft thick. Other veins cut in upper workings are not recognized on lower levels, regardless of faulting, and mineralized structures encountered underground may be absent on the surface. The lower extremities of some major veins are conspicuous, sulfide-rich quartz stockworks. Blind vein apices are apparently marked by strong silicification which merges with less replaced wall rock.

Dip of the veins decreases radically with depth. At the surface, nearly all veins dip 65° to 75° west. On the Friedman level vein dips rarely exceed 20° west and parts of the Blizzard 2 vein (?) are nearly flat lying (sections A-A′ and B-B′, Fig. 5). Veins maintain a steeper attitude toward the north, regardless of depth.

The major veins have been stoped to a vertical depth of more than 1,000 ft below the summit of Nenzel Hill. They have been mined for combined strike lengths of 1,500 ft on the East vein and over 1,650 ft along the West vein. Because of decreasing dip, more than 1,500 ft of the West vein and 1,800 ft of the East vein have been mined downdip. In places, internal silicified wall rock and gouge in addition to veins were mined as ore. Grades were typically erratic but generally declined from 30+ oz Ag/ton in near-surface stopes to <10 oz Ag/ton below 1,000 ft. Production from the veins declined markedly with depth.

Postmineralization faulting coincident with major veins is manifested by crushed zones of quartz and wall rock paralleling vein margins. Displacement along vein faults varies from a few feet to tens of feet, but pre- and postmineralization components are difficult to separate.

Myriads of faults and fractures in Weaver and Rochester rocks are observed underground. The majority of these strike within 30° of north and dip 60° or less west. They appear to be largely coplanar with major vein faults but may be sympathetic with west-dipping early Tertiary (?) structures which have intricately displaced Triassic rocks along the eastern flank of the Humboldt Range (Fig. 2). The thorough fracturing has allowed deep penetration of ground water. Abundant sulfides remain only in veins and silicified rhyolite on lower mine levels.

Vein mineralogy

Two stages of vein mineralization occur at Nenzel Hill. Stage 1 veins, found only at depth on the Friedman and Pitt levels, consist of coarse-grained, euhedral quartz, K-feldspar, and sulfides. Individual sulfide crystals are commonly 0.5 in. on edge. The veins are slightly vuggy, <2 in. thick, and have sharp, planar contacts with wall rock. They apparently filled well-defined open fractures.

All precious metal production has come from stage 2 quartz - K - feldspar - sericite - sulfide - sulfosalt veins which are localized in fissures formed during extensive high-angle faulting. Most stage 2 mineralization has marginally or completely replaced fragments of brecciated rhyolite in fault zones. The scarcity of silicified relict wall-rock fragments; the overall microcrystalline, granular texture of epigenetic quartz; and the lack of vugs, mineral zonation, crustification, and intramineralization brecciation suggest that much of the matrix in the fault zone was gouge or very fine-grained material that was replaced by silica. Stage 2 vein formation apparently took place as a single, continuous physical-chemical event. Stage 2 veins cut stage 1 veins on the Friedman level.

Sulfide minerals bear no obvious relationship to quartz grain size or position relative to breccia fragments and enclosing wall rock, but there is a tendency for sulfides and sulfosalts to cluster in small aggregates, imparting a mottled appearance to some vein mineralization. Individual sulfide grains in stage 2 veins rarely exceed 0.1 inches in maximum dimension.

Quartz, K-feldspar, sericite, and clay minerals are the only nonsulfide vein constituents. Quartz comprises more than 90 percent of all veins. K-feldspar occurs in both stage 1 and stage 2 mineralization where it is intergrown with pyrite, sphalerite, and galena. A (minimum?) K-Ar age of 57.9 m.y. was determined for stage 2 K-feldspar from the Friedman level (Table 3A).

Unoriented laths of sericite, up to 200 microns long, are commonly intergrown with pyrite in stage 2 veins. Most of the mica grains are several times larger than microcrystalline aggregates of sericite developed from feldspar alteration in wall rocks. Seams and pods of finer grained, white sericite become increasingly abundant in major veins near the surface and are profuse in sections of the Big Chief vein on the Crown Point level (Fig. 5). A K-Ar age of 85.7 m.y. was determined for this sericite (Table 3A).

X-ray and infrared analyses reveal no clays mixed

TABLE 3A. K-Ar Ages of Rock and Hydrothermal Phases from the Humboldt Range

Sample no.	Description and location	Mineral dated	K-Ar age (m.y.)	Reference
F-22	Quartz-K-feldspar-sulfide vein, Friedman level, Nenzel Hill	K-feldspar	57.9 ± 2.9	(1)
BCV-1	Quartz-sericite-sulfide vein, Crown Point level, Nenzel Hill	sericite	85.7 ± 4.3	(1)
—	Intrusive quartz monzonite, Rocky Canyon	biotite	71.4 ± 3.0	(2)
—	Quartz-K-feldspar vein, Black Canyon mine	K-feldspar	73.2 ± 2.0	(2)
LO-1	Quartz-sulfide-gold vein, Looney mine, lower Rochester Canyon	sericite	72.5 ± 2.2	(3)
CM-1	Quartz-sericite-dumortierite vein, Champion mine, Rolands Canyon	sericite	73.7 ± 2.2	(3)
OF-SD	Quartz-sericite-andalusite-dumortierite schist, Tate's Prospect, High Grade Canyon	sericite	77.6 ± 2.3	(3)
NP-CA	Quartz-sulfide vein, Nevada Packard mine	sericite	78.8 ± 2.4	(3)

Locations of deposits and occurrences with sample designations are shown in Figure 2.
(1) This paper (anlayses by Teledyne Isotopes)
(2) Silberman et al., 1973
(3) Vikre, 1977 (analyses provided by M. L. Silberman, U.S. Geological Survey)

TABLE 3B. Probability Levels of Age Differences between Sericite Samples from the Rochester District

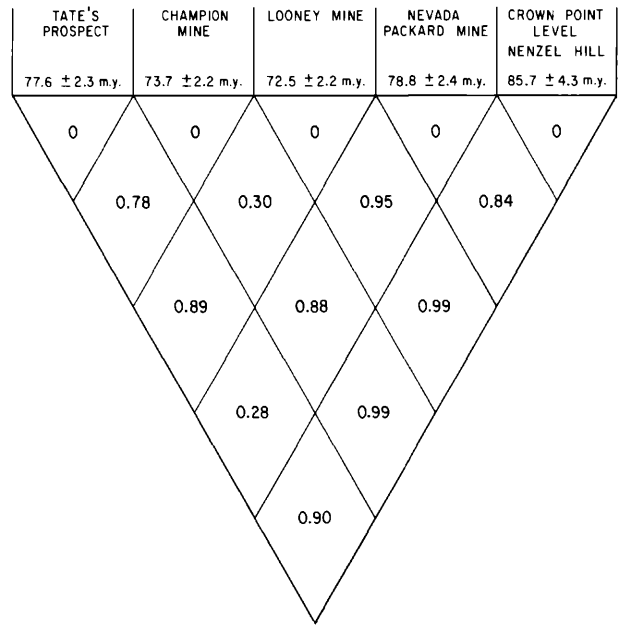

with hydrothermal sericite. Minor amounts of supergene kaolinite and poorly crystalline sericite occur in postmineralization fault zones and weathered fractures. White resilient-textured halloysite in stage 1 veins on the Pitt level probably formed by weathering of K-feldspar.

Sulfur-bearing minerals include, in approximate order of abundance: pyrite, sphalerite, argentian tetrahedrite, arsenopyrite, chalcopyrite, galena, covellite, chalcocite, stromeyerite, polybasite, pyrargyrite, acanthite, pyrrhotite, teallite, and owyheeite. Gold as electrum is a minor constituent. Pyrite comprises more than 95 percent of all sulfides but no more than a few percent of any vein. Pyrrhotite, teallite, and owyheeite are exceedingly rare. Argentian tetrahedrite is the most important hypogene silver-bearing phase. Oxidation of primary sulfides and sulfosalts has produced chlorargyrite, embolite, silver, chalcophanite, jarosite, melanterite, anglesite, manganese oxides, amorphous iron oxides, hematite, goethite, and chalcanthite, the latter three in noticeable amounts.

Paragenetic relations among epigenetic species in stage 2 veins are summarized in Figure 6. Most hypogene sulfides are contemporaneous, although arsenopyrite and pyrrhotite may predate all others. Arsenopyrite is invariably euhedral and contains no inclusions of other sulfides or sulfosalts. It is often spatially associated with electrum. Pyrrhotite occurs in both stage 1 and stage 2 veins but is nearly entirely replaced by pyrite and sphalerite. Copper sulfides and many of the silver-bearing phases are, in part, para-

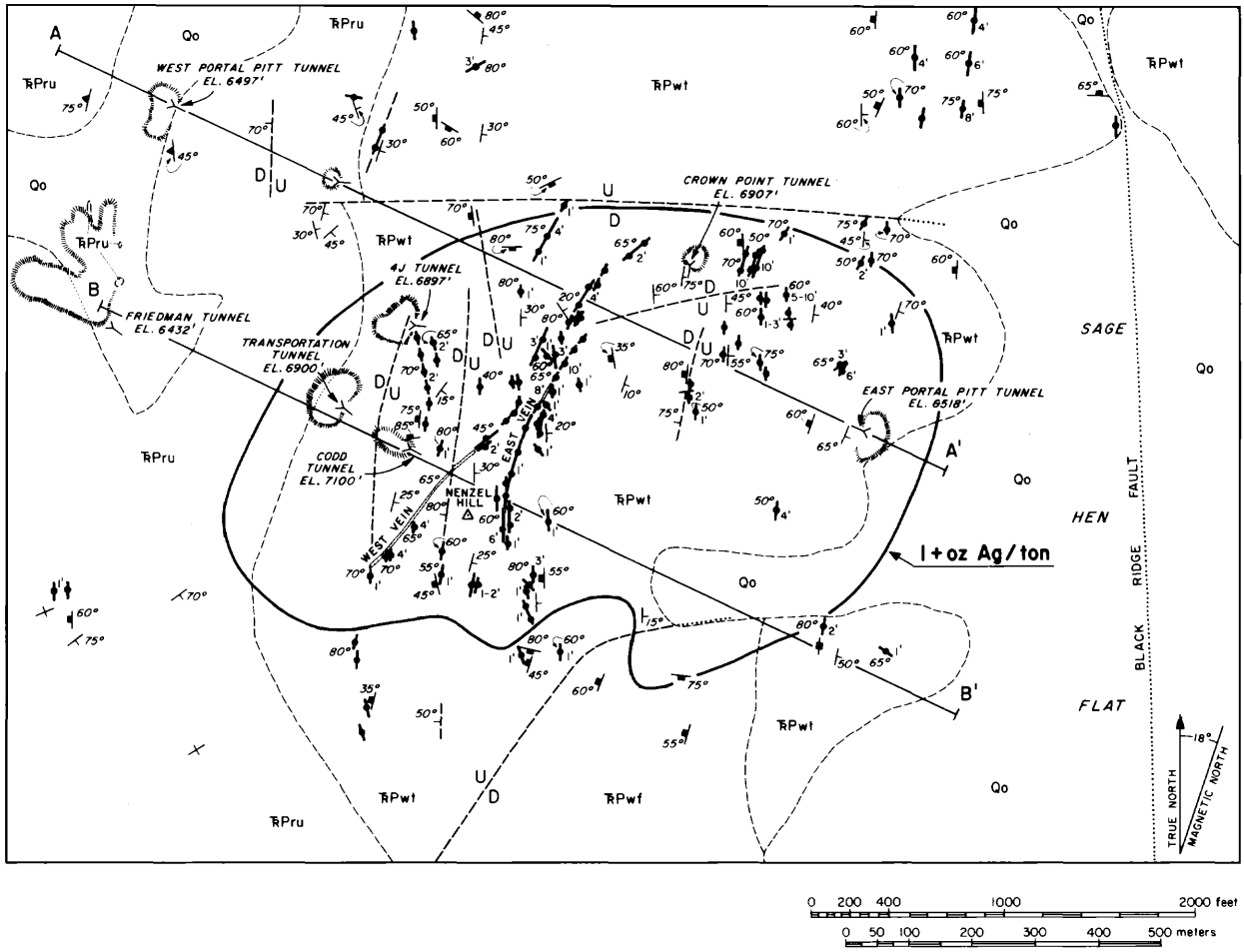

FIG. 5. Geologic map and sections of Nenzel Hill.

genetically late. Tetrahedrite, pyrargyrite, and polybasite occur as intergrowths and inclusions in other sulfides but also concentrically replace earlier deposited species. Marginal replacement textures suggest that quartz deposition may have persisted after the crystallization of all other hypogene sulfides.

Forms of low-grade mineralization

The low-grade silver deposit crops out on the east slope of Nenzel Hill (Fig. 5). Its lateral boundaries are both gradational and structural. The southern and eastern margins of the deposit are faulted and concealed by colluvium. The western and northern borders are mainly a function of grade. The vertical extent of mineralization is variable and ore will ultimately be defined by grade and open-pit economics. Drilling has outlined several higher grade zones within the deposit. Significant gold values are also recoverable.

The silver distributed throughout large volumes of rhyolite at Nenzel Hill has three sources: primary silver minerals in quartz-silicate-sulfide-sulfosalt veins, silver in wall-rock pyrite, and silver in supergene phases. The latter occurrence is derived from weathering of hypogene sources and includes an estimated 80 percent of all low-grade silver mineralization.

Quartz-silicate-sulfide-sulfosalt veins in the low-grade deposit vary from structures less than 0.05 in. wide and a few inches long, which are discernable only under the microscope, to veins more than 3 ft thick and hundreds of feet long. The thick or major veins were the sites of the former production referred to previously. The mean width of all veins is probably less than 0.1 in. and veins less than 0.05 in. thick in unoxidized rock are difficult to see with the unaided eye. Differential concentrations of limonite in oxidized veins and wall rock emphasize the presence of ultra-thin veins.

The frequency of veins is markedly skewed toward thinner veins, and thick veins are rare by comparison.

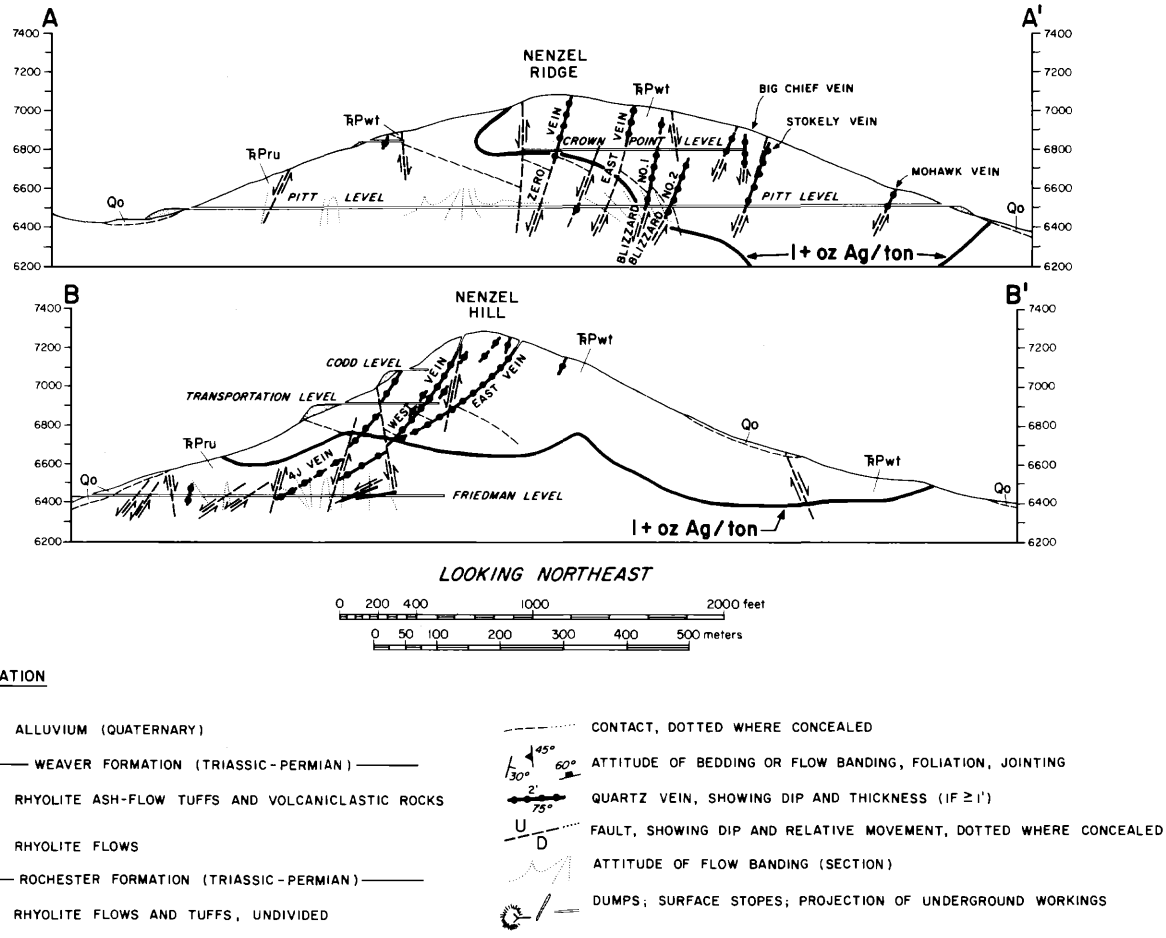

FIG. 5—(*Continued*)

In general, the abundance of narrow veins is greater adjacent to thick veins, and low-grade mineralization is best developed where major veins are abundant and closely spaced. Although major veins are fairly consistently oriented (Fig. 5), veins less than a few inches in width fill random fractures.

Unweathered veins of all sizes which contain hypogene sulfides make up no more than 15 percent of the low-grade mineralization. A visual correlation of veins with grade is evident, but sulfide oxidation, postdepositional movement of silver, and difficulty in recognizing all mineralized veins inhibit accurate grade prediction except by assay. Samples of hypogene vein mineralization are shown in Figure 7.

Pyrite disseminated in wall rocks contributes, at most, 5 percent of the silver grade. Its characteristics were discussed previously in the section dealing with pyrite regionally distributed in Koipato rhyolites. Precious metal abundances in wall-rock pyrite from Nenzel Hill are listed in Table 1. Wall-rock pyrite occurs in optically homogeneous cubes which are less than 30 μm on edge. It is rather evenly distributed regardless of vein proximity and forms 1 to 5 volume percent of the rhyolites. The preferred association of pyrite with sericite and quartz in altered phenocrysts and rock fragments has been previously described. Wall-rock pyrite is nearly always cubic. It is much finer grained than the aggregates which characterize vein sulfides, and it is free of visible inclusions. Occasionally pyrite shares cubic cavities with anatase (?), suggesting pseudomorphic replacement of titanium-bearing, primary iron oxides. Microprobe beam traverses across disseminated pyrite cubes suggest that silver occurs evenly distributed in the matrix and as point concentrations of suboptical silver-bearing inclusions.

Weathering

Numerous phases have been deposited by ground water in the extensively fractured rhyolites of Nenzel

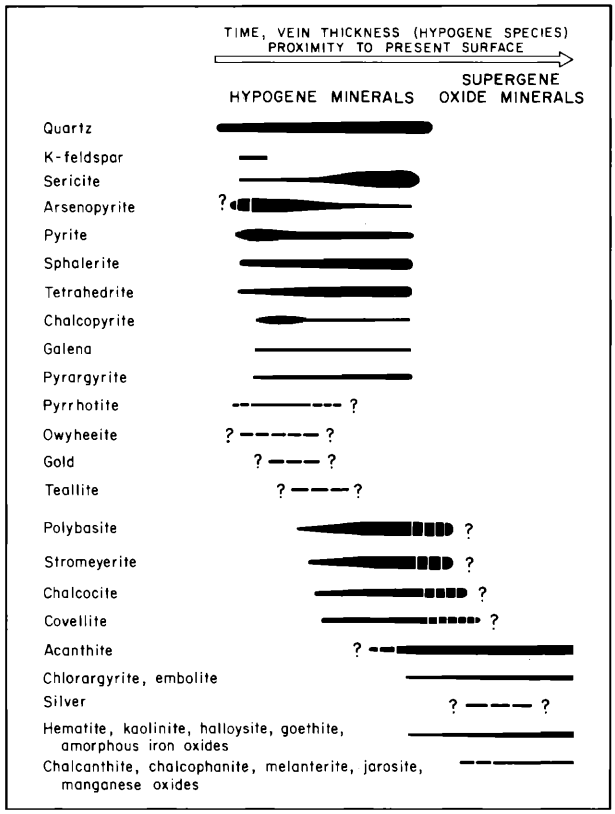

FIG. 6. Probable paragenetic relations in stage 2 veins in Nenzel Hill. Line thickness denotes changing abundance but has only a general relation to the abundance of the other phases.

Hill, and the majority of low-grade silver occurs in supergene sulfide, both oxidized and partly oxidized forms. Textures, distribution, and occurrences of acanthite, silver, and silver halogenides, suggest that these phases largely precipitated during weathering. Scanning electron beam imagery, X-ray diffraction, and spectrographic analyses of oxidized vein and low-grade mineralization reveal other supergene silver minerals and occurrences. Limonitic veins and fractures contain, in addition to the silver phases named above, silver-bearing amorphous iron oxides, argentojarosite, silver-antimony-sulfur phases, and silver-copper-sulfur phases. Some silver associations in oxidized veins and fractures are shown in Figure 8.

The origin of some silver sulfosalts is ambiguous, but vein alteration assemblages indicate that copper sulfides are probably not hypogene. Silver sulfosalts may be both hypogene and supergene. Extensive drilling and sampling at Nenzel Hill have defined no significant enrichment of low-grade mineralization. Precious metal values in sulfide-bearing and oxidized rhyolite are similar. Ground water-saturated, permeable, postmineralization fault zones, which are often coplanar with major veins, may contain silver abundances several times those of unweathered veins and are undoubtedly enriched. The elevated grades of near-surface vein assemblages, however, do not necessarily support enrichment as proposed by Knopf (1924) and silver in Nenzel Hill veins probably closely reflects primary hypogene dispersion.

The absence of large-scale silver enrichment is somewhat predictable from examination of oxidized silver phases. The erratic distribution of native silver, chlorargyrite, bromargyrite, and acanthite in Nenzel Hill indicates that weathering conditions fluctuated considerably. All four minerals may be present in a hand specimen, suggesting locally variable oxidation potential and acidity in ground water (Garrels and Christ, 1965; Rose, 1976). In much of the deposit weathering has not progressed beyond in-place oxidation of individual sulfide grains and aggregates (Fig. 8A). Oxidized portions of the deposit are thus considerably out of equilibrium.

Acanthite and chlorargyrite are the most abundant silver phases in the zone of sulfide weathering. The scarcity of native silver in weathered rhyolite in which pyrite is completely oxidized suggests that chlorine activity was high ($>10^{0.3}$ m) during oxidation of sulfides and that much weathering has taken place in a rather acidic environment (Schmitt, 1962; Rose, 1976). Eh was far more influential than pH in producing the existing assemblage.

FIG. 7. Hypogene stage 2 vein mineralization in Nenzel Hill.

A. (a) Stokely vein on the Pitt level (760 ft below the top of Nenzel Hill) consisting of angular fragments of Weaver ash-flow tuff in a quartz-sericite-sulfide-sulfosalt matrix; (b) East vein, Codd lease, containing a similar sulfide assemblage but in different abundances and modes (Fig. 9).

B. Low-grade quartz-sericite-sulfide-sulfosalt stockwork in the Weaver (a,c) and Rochester (b) Formations, Pitt level. Silver-bearing phases are largely restricted to veins and occur mainly as inclusions in pyrite.

C. Photomicrograph of argentian tetrahedrite (tt) and pyrargyrite (pa) in pyrite (py) from the Mohawk vein, Pitt level.

D. Scanning electron beam imagery of inclusions in pyrite from the Blizzard 2 vein, Pitt level, showing elemental distribution of iron (FeKα), sulfur (SKα), lead (PbMα), silver (AgLα), antimony (SbLα), copper (CuLα), and gold (AuMα). This image (and the images in Figure 8) was obtained by photographically recording the distribution of emitted X-ray radiation which, for each element exposed to the electron beam, has a characteristic wavelength.

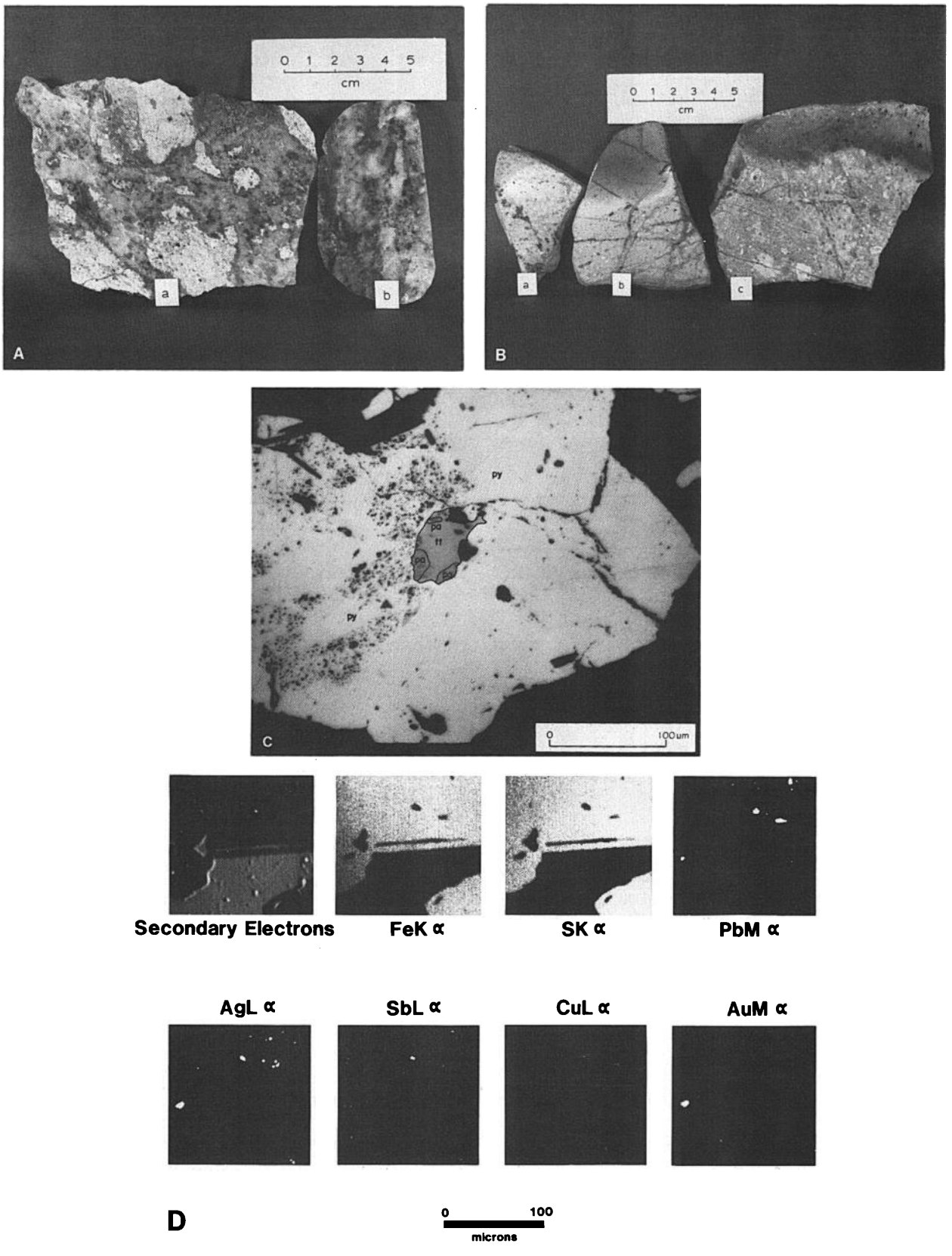
0 1 2 3 4 5
cm
a
b
A
0 1 2 3 4 5
cm
a
b
c
B
py
po
tt
py
C
0
100um
Secondary Electrons
FeK α
SK α
PbM α
AgL α
SbL α
CuL α
AuM α
D
0
100
microns

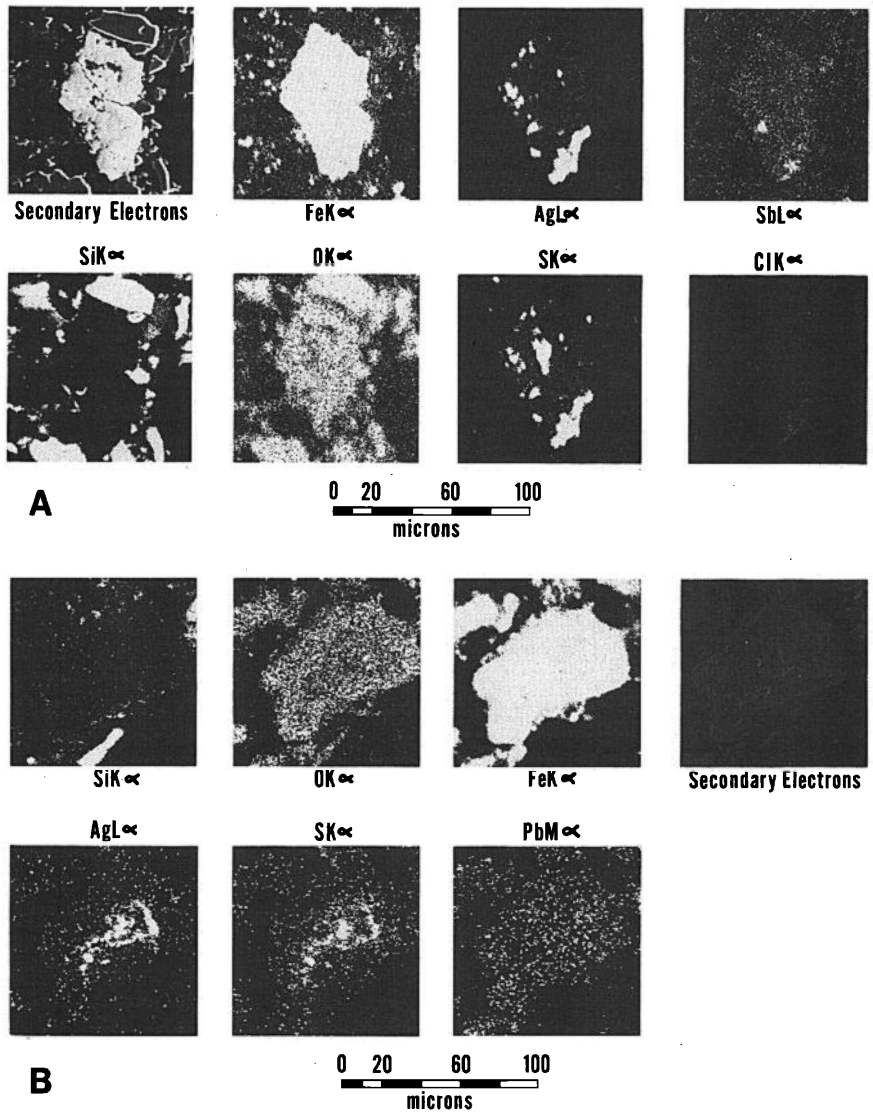

FIG. 8. A. Scanning electron beam imagery of partly oxidized pyrite in quartz from the Blizzard 2 vein, Pitt level, showing elemental distribution of iron (FeKα), silver (AgLα), antimony (SbLα), silicon (SiKα), oxygen (OKα), sulfur (SKα), and chlorine (ClKα). Inclusions of silver-bearing phases in pyrite are common hypogene textures. Such in-place weathering characterizes most of the Nenzel Hill low-grade mineralization.

B. Scanning electron beam imagery of a quartz-iron oxide-acanthite intergrowth from an unnamed vein, Pitt level, showing elemental distribution of silicon (SiKα), oxygen (OKα), iron (FeKα), silver (AgLα), sulfur (SKα), and lead (PbMα). Concentric layering does not resemble any hypogene sulfide textures and is indicative of local silver redistribution by weathering.

Radiometric dating

Because the precious metal deposits in the Rochester district cannot be closely dated by stratigraphic or structural relations, several K-Ar ages on vein and other hydrothermal silicates were determined by Dr. M. L. Silberman of the U. S. Geological Survey, Menlo Park, California, and by Teledyne Isotopes, Westwood, New Jersey. The deposits dated include Nenzel Hill, Nevada Packard, a gold-bearing vein, and stratiform dumortierite occurrences (Table 3A). All but the Nenzel Hill dates are in general agreement with the somewhat questionable age of 71.4 ± 3 m.y. determined for biotite from the Rocky Canyon stock (Silberman et al., 1973). The relatively young age of K-feldspar from Nenzel Hill may have resulted from argon leakage. The feldspar has a maximum microcline structure, which does not retain argon well and the age should be considered minimal (M. L. Silberman, pers. commun.). Because the area has undergone a complex thermal history since eruption of the Koipato volcanics, it is possible that both the dated

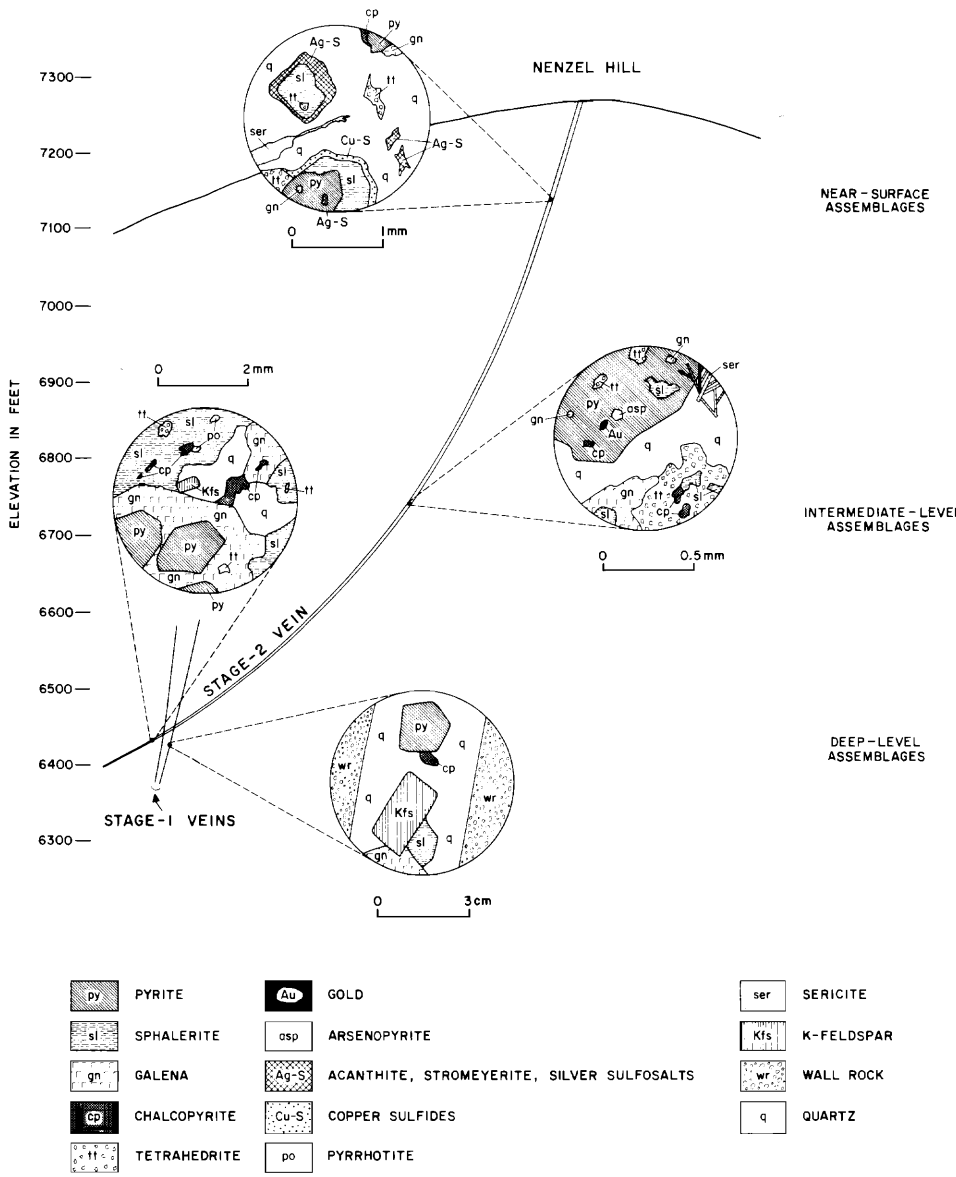

FIG. 9. Diagrammatic portrayal of time-space relationships among stage 1 and stage 2 vein assemblages in Nenzel Hill.

minerals and the Rocky Canyon biotite have been reset by postcrystallization argon loss (Hanson and Gast, 1967; Hart, 1964).

The possibility of argon leakage and the resetting of sericite and K-feldspar ages require that several hypotheses be considered for the age of mineralization. The explanation favored in this paper relates the precious metal (samples F-22, BCV-1, LO-1, and NP-CA, Table 3A) and dumortierite mineralization (samples CM-1 and OF-SD, Table 3A) to Late Cretaceous plutonism in the Humboldt Range. Stratigraphic reconstruction, the ages and relations of all intrusives to alteration and stratigraphy, fluid inclusions, and geochemical and stable isotope data strongly suggest that mineralization in the district formed considerably later than the Permian-Triassic Koipato volcanic event. Overlapping K-Ar ages of most of the vein deposits and the dumortierite mineralization suggest that at least some of the veins formed during a hydrothermal event which partly coincided with extensive development of schistosity along the western flank of the Humboldt Range.

The K-Ar age data imply a range in age of vein development of over 13 m.y., which is long relative to the documented duration of vein and alteration episodes in epithermal ore deposits (Silberman et al., 1979). Table 3B is a statistical summary which gives levels of probability of age differences among the

TABLE 4. Compositions of Sphalerite, Arsenopyrite, and Pyrrhotite in the Nenzel Hill Mineralization, Determined by Microprobe

Location (elevation in feet)	Sample number, site	Zn	S	Cd	Mn	Fe	Total	Mole % FeS
Sphalerite								
East, West veins (~7,000–7,200)	AD-15	69.5	33.0	0.12	0.02	0.86	99.90	1.6
Stage 2	RMD-EV, 1a	64.5	33.4	<0.10	<0.02	1.00	98.90	1.8
	RMD-EV, 1b	65.9	32.7	<0.10	<0.02	1.02	99.62	1.8
	RMD-EVI, 1	65.1	33.1	0.14	<0.02	1.80	100.14	3.2
	RMD-EVI, 2	64.2	32.4	0.12	<0.02	1.54	98.26	2.6
	152, 1	64.3	33.0	0.18	0.02	2.16	99.66	3.9
	152, 1a	66.4	32.9	<0.10	<0.02	1.74	101.04	3.1
	RD78-3, 1	64.9	33.3	0.17	—	2.37	100.74	4.2
	RD78-3,2	64.4	32.8	0.16	—	1.63	98.99	2.9
Intermediate levels (6,782–6,956)	24, 1	66.4	33.0	0.26	<0.02	0.30	99.96	0.6
Stage 2	24, 2	66.1	32.7	0.20	<0.02	0.22	99.22	0.5
	RD78-6, 1	65.0	32.3	0.21	—	1.06	98.57	1.9
	RD78-6, 2	66.1	32.7	0.12	—	0.99	99.91	1.8
	RD78-1, 1	65.5	32.7	0.14	—	0.41	98.75	0.7
	RD78-1, 2	64.5	32.9	0.18	—	1.43	99.01	2.6
	116	65.6	33.0	0.25	0.03	1.39	100.27	2.5
	AD-8, 1	65.0	33.1	<0.10	<0.02	2.10	100.20	3.8
	AD-8, 2	65.0	33.1	<0.10	<0.02	1.89	99.99	3.4
	AD-8, 3	65.3	33.3	<0.10	<0.02	2.07	100.67	3.8
	AD-8, 1b	63.7	33.0	<0.10	0.02	1.87	98.59	3.3
	AD-8, [2]	64.2	32.9	0.19	<0.02	1.87	99.16	3.3
	RD78-8, 1	63.3	32.3	0.19	—	2.06	97.82	3.7
	RD78-8, 2	64.4	32.7	0.23	—	1.03	98.63	2.3
	RD78-7, 1	64.3	33.0	0.27	—	2.42	99.99	4.3
	RD78-7, 2	65.3	33.3	0.31	—	2.36	101.27	4.2
	57W415	64.6	32.9	0.14	<0.02	2.27	99.91	4.1
	4JV, 1	64.0	31.1	<0.10	0.03	3.16	98.29	5.7
	4JV, 2	63.4	33.0	0.21	0.03	2.73	99.37	4.9
	RD78-4, 1	63.5	33.2	0.14	—	3.33	100.17	6.0
	RD78-4, 2	64.0	33.2	0.18	—	2.77	100.15	5.0
Pitt level (6,518)	(4)124	64.9	32.8	0.18	0.04	0.87	98.79	1.6
Stage 2	P-33, 1	64.4	32.7	0.30	<0.02	1.40	98.80	2.5
	P-33, 2	64.1	32.8	0.20	0.02	1.29	98.41	2.3
	P-33, (2)	65.6	32.8	<0.10	0.02	1.02	99.44	1.8
	SV6-2	64.6	32.6	0.20	0.03	1.21	98.64	2.2
	963	64.6	32.8	0.13	<0.02	1.22	98.75	2.2
	CV-1	64.8	32.9	0.19	0.03	1.31	99.23	2.4
	(3)359, 1	65.0	33.1	0.20	<0.02	1.83	100.13	3.3
	(3)359, 2	65.2	32.7	<0.10	<0.02	1.92	99.82	3.4
	RD78-2, 1	62.0	32.7	0.46	—	3.66	98.82	6.6
	RD78-2, 2	64.6	32.6	0.47	—	1.91	99.58	3.4
	RD78-2, 3	64.3	32.8	0.47	—	2.21	99.78	4.0
	P-29	62.9	33.0	0.37	0.02	2.36	98.65	4.2
	(1)265	63.7	33.0	0.14	<0.02	3.02	99.86	5.4
	P-46, 1	62.6	32.9	0.37	0.03	3.60	99.50	6.5
	P-46, 2	62.8	33.0	0.36	0.04	3.45	99.65	6.1
	(6)122	65.5	31.8	<0.10	—	1.49	98.79	2.6
Friedman level (6,432)								
Stage 2	F-8	60.8	33.2	0.28	<0.02	5.79	100.25	10.7
	F-9b, 1	61.0	33.1	0.24	0.03	5.41	99.78	9.7
	F-9b, 3	60.3	32.9	0.25	0.03	5.45	98.93	9.8
	F-15a	60.7	33.0	0.21	<0.02	5.61	99.52	10.0
	F-18b, 1	60.6	33.1	0.25	0.03	5.87	99.85	11.1
	F-18b, 2	59.7	33.2	0.23	0.03	6.56	99.72	11.7
	F-19b, 1	61.7	33.7	0.22	0.02	5.78	101.42	10.2
	F-19b, 2	59.2	32.5	0.25	0.02	5.72	97.69	10.2
Stage 1	F-12B, 1	59.1	33.1	0.17	0.03	7.02	99.42	12.5
	F-12B, 2	57.9	33.1	0.22	0.08	8.06	99.36	14.4
	F-12B, 3	58.6	33.4	0.18	0.08	7.57	99.83	13.5

TABLE 4—(*Continued*)

Location (elevation in feet)	Sample number, site	Zn	S	Cd	Mn	Fe	Total	Mole % FeS
	F-12C, 1	59.8	33.4	0.22	0.02	6.38	99.82	11.4
	F-12C, 2	59.7	33.2	0.21	0.02	6.43	99.56	11.5
	F-12C, 3	58.0	33.2	0.24	0.09	7.24	98.77	13.0
		As	Fe	S	Co			
Arsenopyrite	AD-8	42.5	35.5	21.8	0.07		99.87	
	AD-12	42.1	36.5	22.2	0.08		100.88	
	AD-15	41.3	35.6	22.5	0.07		99.47	
	(1)265	42.3	35.8	21.9	0.04		100.04	
	CV-1	41.9	36.1	22.5	0.05		100.55	
	116	42.9	35.5	21.8	0.06		100.26	
	4JV	42.7	35..1	22.0	0.08		99.88	
	S-S12	41.0	35.3	21.7	0.07		98.07	
		Fe	S					
Pyrrhotite	F-12B	60.9	39.0				99.9	
	F-15a	59.4	39.2				98.6	
	NP-A, 1	60.0	38.3				98.3	
	NP-A, 2	59.7	38.1				97.8	

< = not detected; — = not analyzed

All values are mean weight percent based on 5 spot analyses. Matrix effects were corrected by MAGIC-1 and MAGIC-IV. Intrasite variation never exceeded 5 percent of the value reported. Analyses by T. Kartelias, ASARCO Central Research Department, and Vikre (1977).

sericite samples. Probability levels exceed one standard deviation (68%) for nearly all combinations—suggesting that the age differences and ranges have validity. Alternatively, the Mesozoic orogeny may have been more complex than envisioned. A multiple intrusive epoch entailing emplacement of several stocks of slightly differing ages may have generated several temporally distinct hydrothermal events.

Another plausible hypothesis is to consider the Rochester district mineralization a Triassic analogue of some Tertiary veins. Among the Tertiary precious metal deposits in the United States, particulary those in the western Great Basin, a consistent temporal relationship between host-rock deposition and epithermal-type-mineralization has emerged from extensive K-Ar and other radiometric dating. Deposits occurring in volcanic rocks such as Bodie, Tonopah, and Goldfield (Silberman et al., 1972; Bonham et al., 1972; Ashley and Silberman, 1976) invariably formed within a short period, often less than 1 m.y., after cessation of the volcanic event. Thus, a logical genetic assumption for the Rochester district silver and gold veins would place the age of mineralization at approximately 235 m.y. before present, corresponding to the approximate stratigraphic and radiometric age determinations of the hosting Koipato rhyolites. The Cretaceous ages of sericite would therefore have been caused by resetting in thermal aureoles of Cretaceous plutons, such as the Rocky Canyon stock.

The above interpretation might explain the range in ages of the precious metal vein and dumortierite deposits. The age variations may have been due to local temperature differences during the postcrystallization thermal event.

The resetting explanation conflicts with the fact that the veins entirely escaped deformation and recrystallization during the Cretaceous orogeny, even though apophyses of the Rocky Canyon intrusive may lie very close to the surface in the Rochester district (Fig. 4). Oxygen isotope temperatures suggest that the dumortierite mineralization crystallized at higher temperatures than did any of the vein mineralization. Argon loss, which is correlative with increasing temperature, should make the stratiform dumortierite mineralization the youngest, which it is not. Thus, argon depletion conflicts with the results of Table 3A.

Sulfide-Silicate Zoning

Spatial, modal, and temporal relations among hypogene minerals in stage 1 and stage 2 veins in Nenzel Hill are summarized in Figure 9. These relations were determined by extensive microscopic examination and microprobe analyses. Silicate zoning in both stages is manifested by a quartz + K-feldspar assemblage in the lowest vein extremities. Stage 2 mineralization is dominated by a quartz + sericite assemblage in wider, near-surface vein segments. K-feldspar occurs only in mineralization on the Friedman and

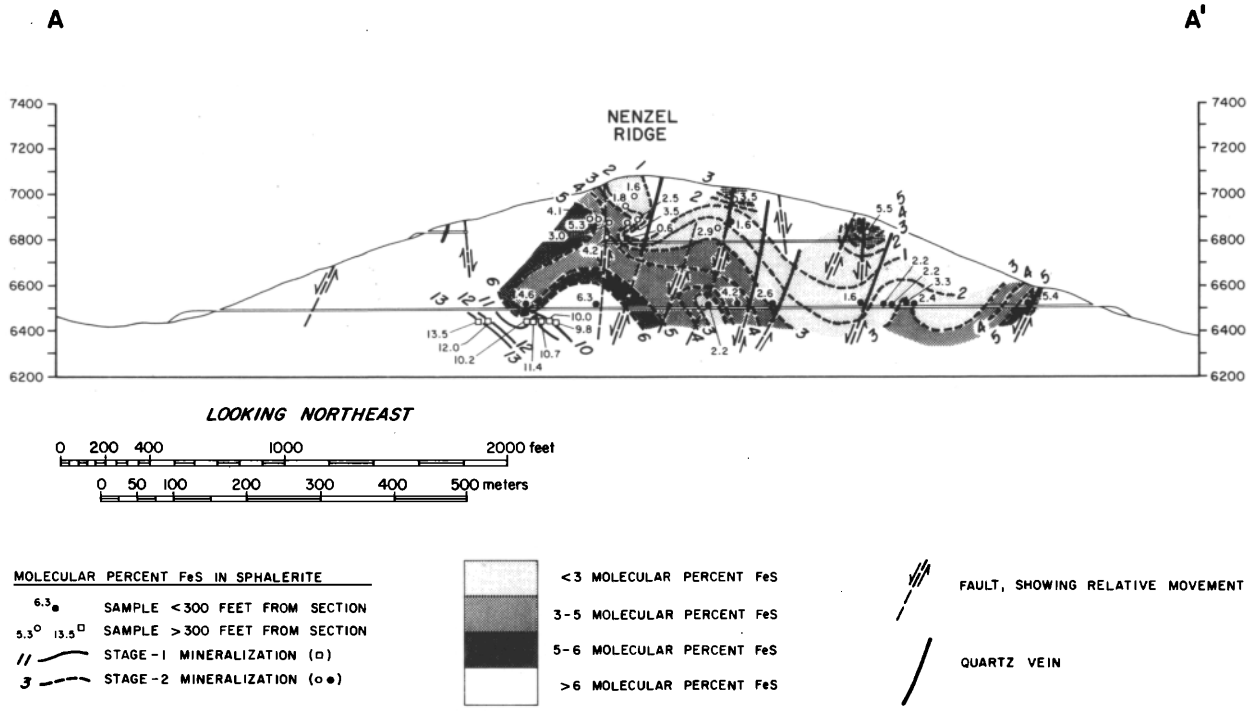

FIG. 10. Mole percent FeS in sphalerites in Nenzel Hill mineralization, projected on to section A-A' from Figure 5. Sample values averaged from 61 analyses in Table 4. Data suggest that sphalerites become progressively iron poor at higher stratigraphic levels.

Pitt levels. Sericite becomes increasingly abundant toward the present surface. Its mode changes from relatively coarse-grained intergrowths with sulfides at depth to irregular microcrystalline pods and thin seams in quartz with increasing elevation.

Sulfide zoning is more complex and nearly all phases show transgressive habits and abundances. Boundaries between assemblages shown in Figure 9 are very indistinct and assemblages merge over hundreds of feet. On the Friedman level, up to 10 percent of the veins are coarse-grained intergrowths of galena, sphalerite, and pyrite. Inclusions of argentian tetrahedrite are sparse, but pyrrhotite is relatively common. With increasing elevation and vein width, galena and sphalerite abundances sharply decrease, total vein sulfide content drops to a few percent, and pyrrhotite disappears. The assemblage pyrite + silver sulfosalts replacing sphalerite predominates in upper thicker vein segments. The change is gradational and veins on intermediate levels are characterized by pyrite + sphalerite aggregates with prolific sulfide and silver-sulfosalt inclusions and intergrowths.

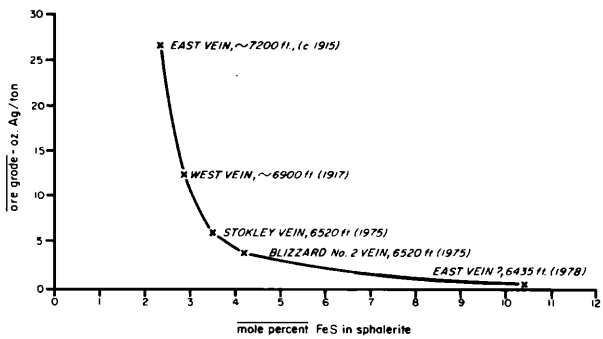

FIG. 11. Average mole percent FeS in sphalerites from the major veins in Nenzel Hill, plotted against the average silver grade of the sphalerite-bearing vein segment. Sphalerite compositions are from Table 4. Vein segment grade averages were provided by ASARCO Inc. Data suggest that the abundance of silver phases (e.g., grade) was controlled by evolving hypogene processes, if it is assumed that sphalerite composition is a reliable record of FeS activity in hydrothermal fluids.

Average silver in the veins increases from less than 2 oz/ton in the deep level galena + sphalerite + pyrite assemblage to about 6 oz/ton in intermediate level vein assemblages. Near-surface silver sulfosalt-rich vein segments frequently contain more than 30 oz Ag/ton. The iron content of sphalerite in veins also shows vertical and stratigraphic control. FeS in sphalerite (Table 4), displayed on a vertical section through the Nenzel Hill vein system, illustrates the correlation between sphalerite compositions and vein sulfide assemblages (Fig. 10). Both stage 1 and stage 2 sphalerites on the Friedman level are relatively iron-rich and contain 8.5 to more than 11 mole percent FeS. Intermediate level sphalerites contain approximately 3 to 7 mole percent FeS. Iron-poor sphalerites composed of less than 3 mole percent FeS occur with

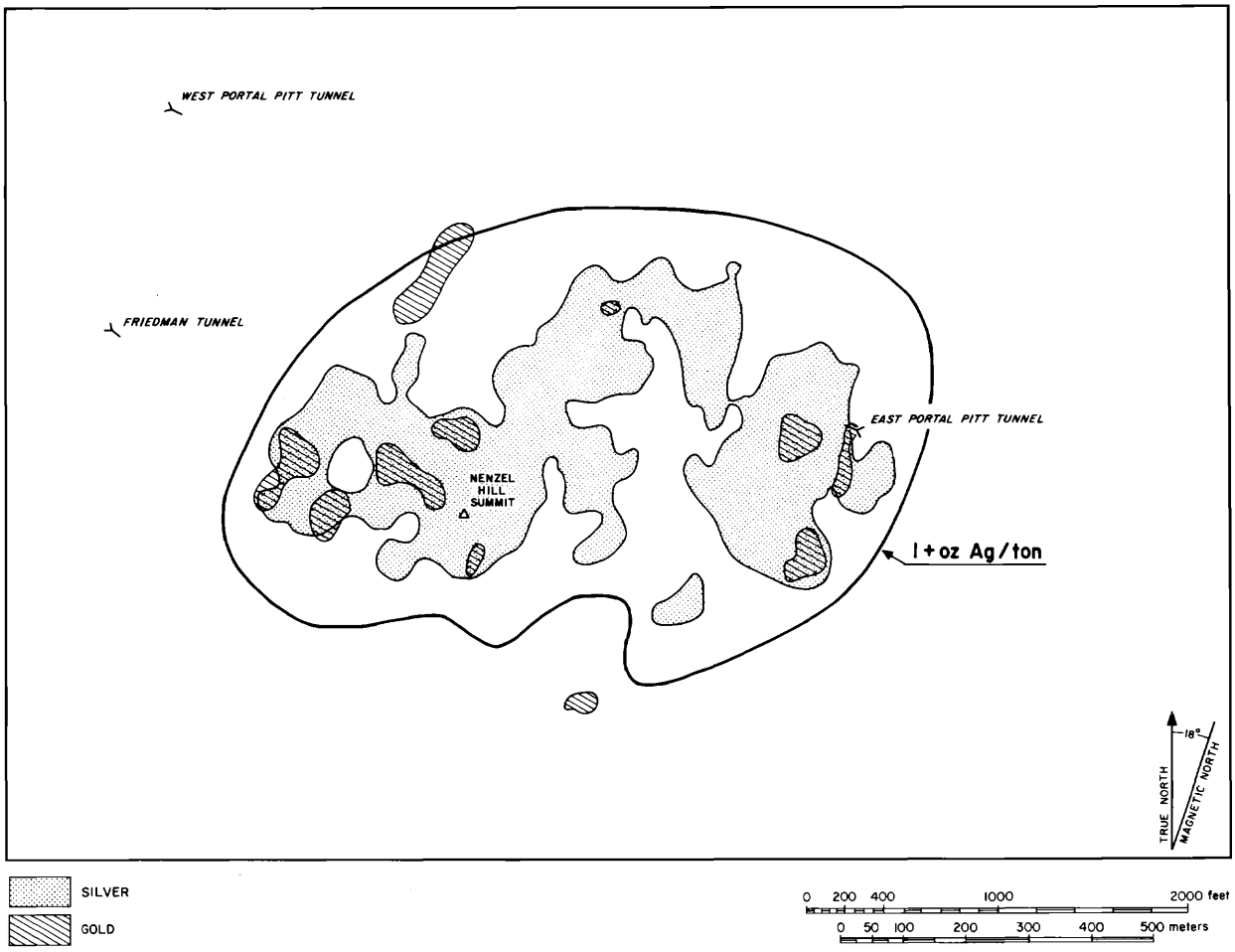

FIG. 12. Slightly modified, computer-drawn plan showing the distribution of higher grade silver and gold mineralization in Nenzel Hill, with silver 100 times more abundant than gold. Data were projected from vertical drill holes and suggest that gold is relatively abundant at the margins of the silver deposit. Area of drawing is the same as Figure 5.

near-surface silver sulfosalt mineralization. Sphalerite composition plotted against average vein grade (Fig. 11) is also indicative of metal zoning and suggests that the silver grade was controlled by hydrothermal fluids and not by ground water.

Silicate and sulfide mineralogy, and textures in low-grade mineralization encountered on the Pitt level, most closely resemble intermediate level stage 2 vein assemblages (Fig. 9), although there are fewer sulfur-bearing species present. There is a slight tendency for narrow veins within the low-grade deposit to become lead-zinc rich with depth and silver sulfosalt abundances to increase with elevation. The best low-grade mineralization occurs in volcanic rocks of the Weaver Formation. Narrow veins in Rochester rhyolite are numerous but invariably poorer in silver. Vertical zoning is much more pronounced in major veins and smaller veins display a relatively narrow range in silver content regardless of assemblages in proximal large veins. Comparison of Figures 5 (section A-A') and 10 indicates most of the low-grade silver mineralization spatially coincides with low iron sphalerite assemblages.

Silver-gold zoning at Nenzel Hill is evident from the compilation of thousands of drill hole assays. Averaged Ag/Au for mineralized intercepts shows that gold abundance, relative to silver, increases with depth and is greatest in Rochester Formation rocks and peripheral to the low-grade deposit (Fig. 12). Similar precious metal zonation was observed at Tonopah, Nevada (Nolan, 1935), and at Tayoltita, Durango (Smith, 1978). At Tayoltita, higher gold concentrations occur in veins closest to premineralization intrusives.

Temperature, Pressure, and Ore Fluid Composition

Qualitative estimates of depositional temperatures for veins in the Rochester district are provided by oxygen isotopes and by the stabilities and composi-

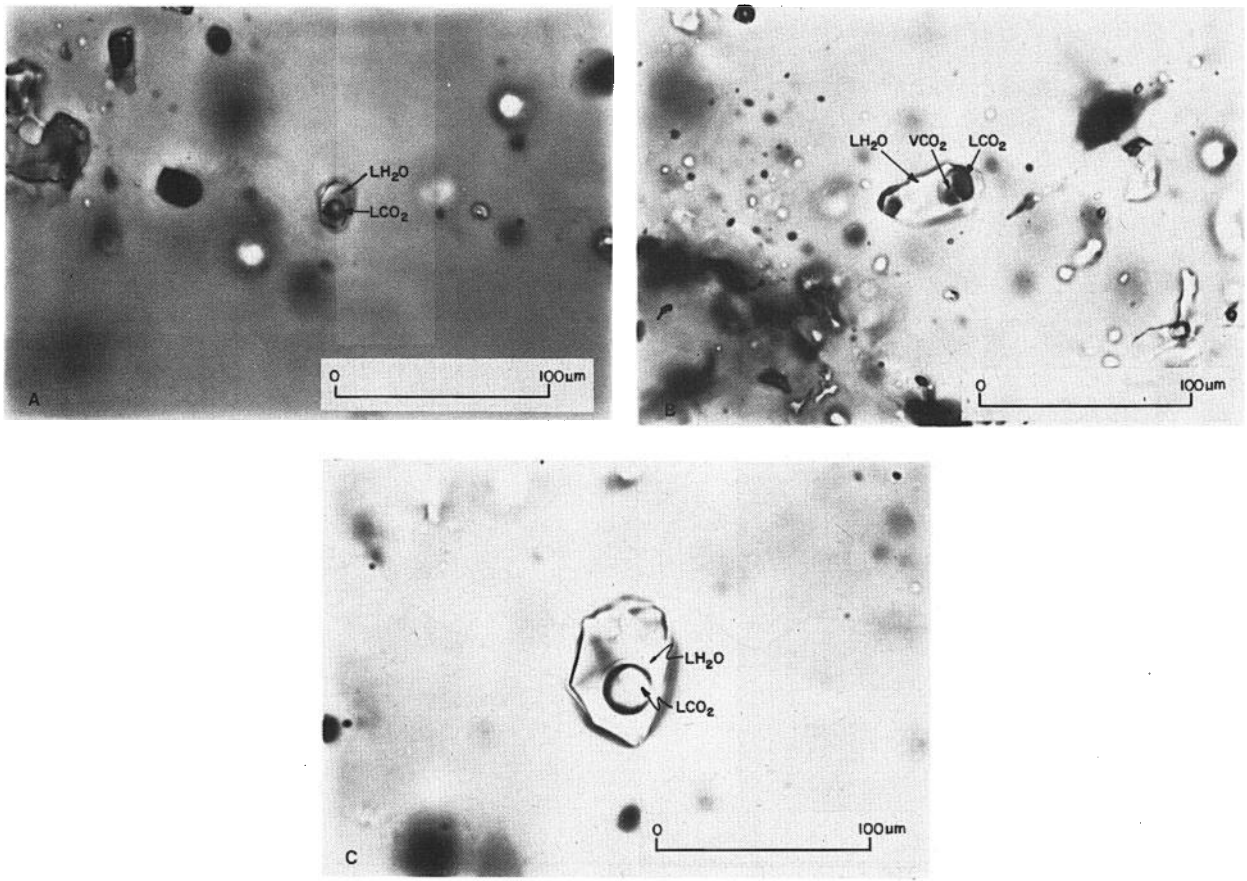

FIG. 13. Primary, three-phase fluid inclusions from silver deposits in the Rochester district, photographed at 23°C. Phases are 1*m* ($Na_{0.843}Ca_{0.075}K_{0.006}Mg_{2.2\times10^{-4}}$)Cl ($LH_2O$); liquid carbon dioxide (LCO_2), and vapor carbon dioxide (VCO_2). Vapor bubble moved too rapidly to be captured on film except in B. All inclusions are in quartz. A. Inclusion from the Blizzard 2 vein, Pitt level, Nenzel Hill. B. Inclusion from the West vein, Rock tunnel, Nenzel Hill. Large CO_2 bubble may be indicative of postdepositional leakage. C. Inclusion from cut A (see Knopf, 1924, plate IV), Nevada Packard mine.

tions of certain hydrothermal minerals. Based on the distribution of O^{18} in coeval sericite and quartz, upper limits on precious metal vein temperatures along the west flank of the range are approximately 500°C. Decomposition of polybasite at ~400°C (Barton and Skinner, 1979) restricts Nenzel Hill stage 2 vein temperatures to less than this value in the latter stages of mineralization. Paragenetically earlier pyrargyrite, which is unstable above 485°C, and intergrowths of pyrite and arsenopyrite, which cannot coexist above 491°C (Barton and Skinner, 1979), also suggest that Nenzel Hill vein temperatures never greatly exceeded 400°C. Coexisting chalcopyrite and hexagonal pyrrhotite in stage 1 mineralization indicate an upper temperature limit of 334°C (Kullerud et al., 1966) if that assemblage is in equilibrium. A lower depositional temperature limit of 265°C for both stage 1 and stage 2 veins at Nenzel Hill is defined by the assemblage pyrite + hexagonal pyrrhotite (Scott and Kissin, 1973).

The composition of arsenopyrite intergrown with pyrite throughout Nenzel Hill stage 2 veins is remarkably constant. It averages $FeAS_{0.91}S_{1.09}$ for eight analyses (Table 4), with variation for any element not exceeding 3 percent of the mean. According to the data of Kretschmar and Scott (1976), arsenopyrite of this composition coexisting with pyrite suggests a depositional temperature of about 370°C.

Fluid inclusions

Fluid inclusions in vein quartz from a variety of deposits in the Rochester district set approximate temperature, pressure, and compositional limits for ore fluids. Resolvable inclusions varied in size from about 5 μm to more than 30 μm. Visual uncertainty, calibration errors, and reproducibility limited the accuracy of homogenization determinations to ±5°C with the available microthermometry apparatus. Errors of up to 3 weight percent NaCl equivalent in freezing point depression determinations resulted mainly from poor visibility. Leakage and decrepitation noted during plate preparation and heating were caused by

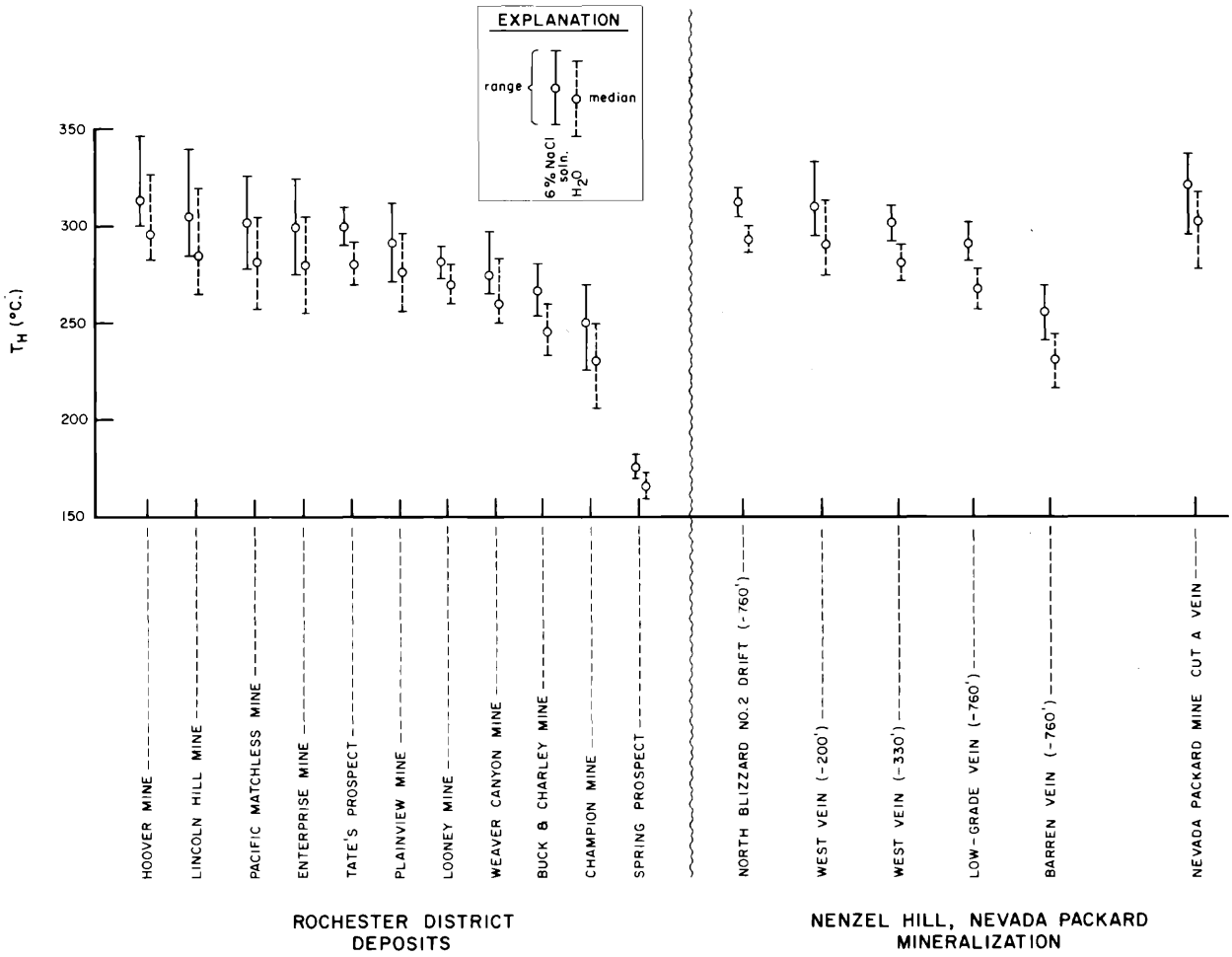

FIG. 14. Pressure-corrected (to 1 kb) fluid inclusion homogenization temperatures (T_H[°C]) for deposits in the Rochester district. Data have been corrected for both pure water and 1*m* NaCl (Lemmlein and Klevtsov, 1961). Only determinations of primary and pseudosecondary inclusions are reported. Data summarize measurements of more than 700 inclusions. Deposit locations are shown in Figure 2.

high internal pressures arising from trapped carbon dioxide phases and the data required careful interpretation (Vikre, 1977). Inclusion types and phase compositions were identified using the criteria of Roedder (1967, 1972) and the data of Kennedy (1954) and Kennedy and Holser (1966).

Remarkably similar morphology and composition among primary and pseudosecondary inclusions are exhibited by the various deposits in the Rochester district, including the Nenzel Hill veins (Fig. 13). Three-phase inclusions contain about 80 volume percent hydrous saline solution (LH_2O),[1] 15 to 22 volume percent liquid carbon dioxide (LCO_2), and 0 to 5 volume percent vapor (carbon dioxide and water). Two-phase inclusions contain 80 to 85 volume percent LH_2O and 15 to 20 volume percent LCO_2, or vapor. All precious metal veins in the Rochester district contain LCO_2-bearing primary inclusions. The morphological difference between three- and two-phase inclusions is either a function of pressure variations during entrapment or, more likely, slight postdepositional leakage.

Consistent phase ratios and compositions among competent inclusions indicate a single-phase hydrothermal fluid, with total pressure greater than vapor pressure, at the time of entrapment. Similarity of phase ratios between widely spaced deposits also suggests a relatively stable temperature and pressure environment throughout the Rochester district at the time of mineralization.

The absence of daughter salts at room temperature in all inclusions indicates that ore solutions contained less than 26 weight percent NaCl. Inclusions suitable for freezing to obtain salinity estimates are scarce and freezing point depression determinations were made on only four vein deposits within the district. The methods and deductions applied to this type of anal-

[1] L = liquid, V = vapor throughout this paper.

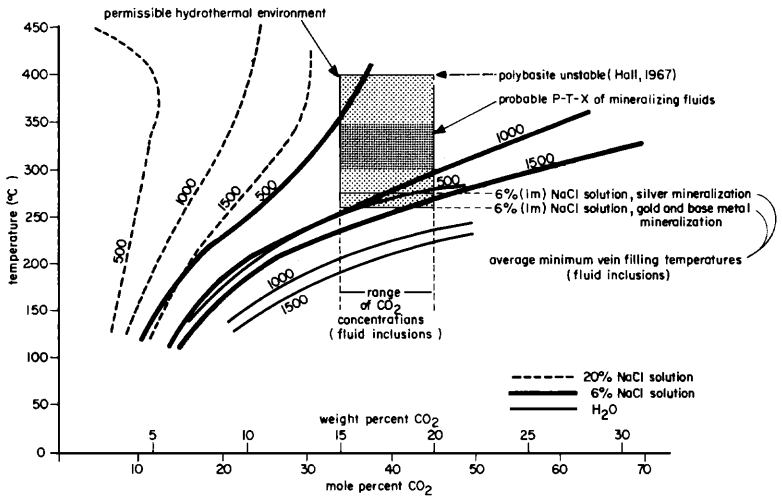

FIG. 15. Isobaric solubility of carbon dioxide in pure water and NaCl solutions of varying salinity (after Takenouchi and Kennedy, 1964, 1965). Numbers above curves denote pressures in bars and are minimum values because the curves represent CO_2 saturation. Stippled area covers probable pressure, temperature, and compositional environment of Rochester district mineralizing fluids.

ysis are described at length by Kelly and Turneaure (1970).

Inclusion salinities range from 2.0 to 8.1 weight percent NaCl equivalent. An average salinity of 6 weight percent NaCl (~1 molal) was assumed for pressure corrections for all deposits. Clynne and Potter (1977) demonstrated that for most natural fluid inclusion compositions, weight percent NaCl equivalent (as determined by the freezing point depression method) is nearly equal to weight percent NaCl.

Analyses of leachate from fluid inclusions in the four samples, coupled with total salinity estimates, provided an average solute composition of $(Na_{0.843}Ca_{0.075}K_{0.006}Mg_{2.2\times10^{-4}})Cl$. The method used, which determines major cation ratios, was modified after that described by Robinson and Ohmoto (1973).

Fluid inclusion homogenization temperatures with pressure and salinity corrections are given in Figure 14. At an assumed precipitation pressure of 1,000 bars and ore fluid salinity of 1 molal NaCl equivalent, corrected homogenization temperatures for all deposits range from 180° to 320°C, and for Nenzel Hill veins average about 300°C—within the temperature range estimated from mineral stabilities and compositions. The effects of carbon dioxide on phase relations in the system H_2O-NaCl-CO_2 oppose those of NaCl, but the effects of salt generally outweigh the influence of CO_2 (Takenouchi and Kennedy, 1965). No temperature corrections have been experimentally determined for this three-component system and, since boiling or exsolution did not occur in any of the deposits, the effects of CO_2 can only be qualitatively estimated. Given the low salinity of the fluid inclusions in the Rochester district ores, the high pressures of formation, and the considerable amounts of carbon dioxide in the original hydrothermal solutions, the carbon dioxide-salt-induced temperature corrections could conceivably be somewhat greater than those estimated on the basis of the two-component H_2O-NaCl system.

Pressure at vein formation

Several lines of evidence suggest that the precious metal mineralization at Nenzel Hill and other deposits in the Rochester district formed at depths considerably greater than those attributed to many silver-gold vein deposits in Tertiary volcanic rocks. By determining the approximate range of filling temperatures of uniform fluid inclusions and the weight percent and fugacities of inclusion components, an estimate of entrapment pressure and depth of mineralization can be derived. Salt solution and carbon dioxide dominate the chemistry of ore fluids and the system H_2O-NaCl-CO_2 closely models the hydrothermal environment. Experimental phase relations indicate that a pressure of about 1,000 bars is consistent with observed fluid salinities, CO_2 concentrations, and inferred entrapment temperatures. Pressures much greater than 1,500 bars or less than 500 bars are improbable for the ore-forming environment, based on fluid inclusion data and Figure 15.

Reconstruction of the post-Koipato section from available exposures in the central part of the Humboldt Range indicates that 2,300 ft of rock overlay what is now Nenzel Hill. However, Tertiary faulting along range margins and consequent graben filling have removed and buried much of the Upper Triassic section. Silberling and Wallace (1969) estimate a composite thickness of nearly 11,000 ft for the Lower to Middle Triassic Star Peak Group and Middle to Upper

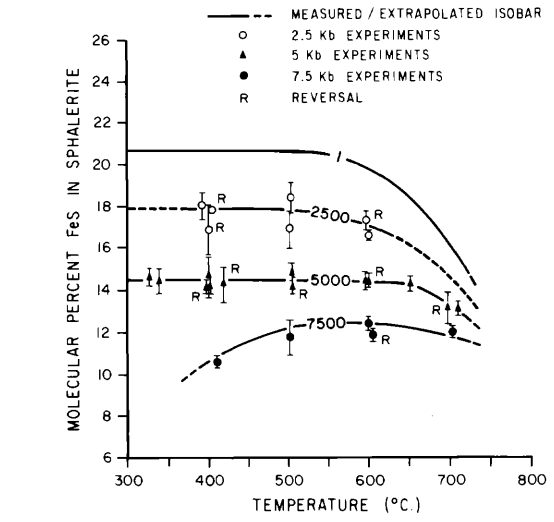

A.

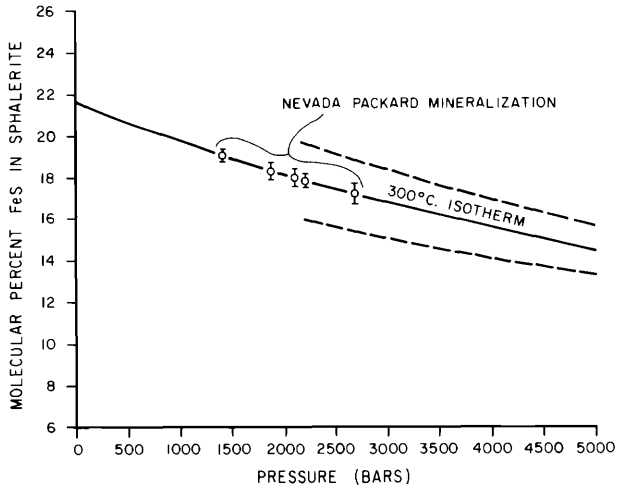

B.

FIG. 16. T-X and P-X projections of the sphalerite + pyrite + hexagonal pyrrhotite solvus isobars and isotherms.

A. Isobaric experimental T-X plots (Scott, 1973). Pressure is in bars. The 1-bar equilibrium curve is from Scott and Barnes (1971) and Scott and Kissin (1973). Width of error bar is one standard deviation of the mean.

B. Isothermal P-X projection derived from A. The range of error in the isobars is shown by dashed lines. Open circles are data derived for this paper and each represents an average of 2 to 3 spot analyses per sphalerite grain. Vertical extensions are the range of analytical error (instrument precision added to maximum variation of standards) per grain.

Triassic "Winnemucca sequence" (Auld Lang Syne Group) in north central Nevada. In addition, at least 1,000 ft of Weaver flows, ash flows, and clastic deposits occur above the deepest extensions of the Nenzel Hill veins. Post-Triassic sedimentation and volcanism could have increased the overburden thickness by the Late Cretaceous, when precious metal mineralization apparently took place. The Nenzel Hill veins and other mineralization in the Rochester district may well have formed at depths exceeding 12,000 ft.

Assuming an average density for post-Koipato carbonate and clastic rocks of 2.67 g/cm^3, lithostatic pressure at 12,000 ft corresponds to more than 980 bars. If hydrostatic pressure predominated in the vein systems, the minimum pressure during ore deposition was about 350 bars.

Isobarically univariant curves for the composition of sphalerite in equilibrium with pyrite and hexagonal pyrrhotite have been determined experimentally by Scott (1973) and Scott and Barnes (1971). Sphalerite, pyrite, and pyrrhotite coexist in apparent equilibrium in hypogene sulfide mineralization at the Nenzel Hill and Nevada Packard deposits (Fig. 2). Enriched vein and stockwork deposits in Koipato rocks were mined for silver at Nevada Packard concurrently with mining at Nenzel Hill, and these deposits are very similar to the Nenzel Hill mineralization (Vikre, 1977).

Pyrrhotite of the assemblage was determined to be hexagonal by chemical and magnetic tests, and by composition. Sphalerites analyzed by microprobe contain from 17.4 to 19.2 mole percent FeS with 3 percent compositional variance. Pyrrhotite studies and sphalerite analyses of Nevada Packard mineralization are described in Vikre (1977). The sphalerites average 18.2 mole percent FeS which corresponds to 1,850 ± 250 bars equilibrium pressure (Fig. 16), or 23,300 ft lithostatic load. Compared to other independent estimates of pressure, sphalerite barometry gives values that are undoubtedly high, although resolution is no better than several hundred bars because of variability of experimental curves. The degree to which the pyrite + pyrrhotite + sphalerite assemblage approached equilibrium is an incalculable factor. Brown et al. (1978) showed that even apparent textural equilibrium does not negate possible chemical zoning or retrograde compositional changes. Furthermore, 300°C may be near the lower useful limit of the sphalerite geobarometer (Browne and Lovering, 1973). However, sphalerites which show no proximity to both pyrrhotite + pyrite in the Rochester district deposits have markedly lower FeS contents and suggest that sphalerite geobarometry has at least general validity.

In conclusion, fluid inclusions, mineral stabilities and compositions, and oxygen isotopes in deposits throughout the Rochester district indicate that temperatures exceeding 300°C but less than 400°C and pressure on the order of 1 kb accompanied mineralization. Similar temperature-pressure estimates derived from widely scattered deposits and ubiquitous quartz-sericite-pyrite alteration suggest that physical gradiants were probably small during hydrothermal mineralization. It is likely that there was little dif-

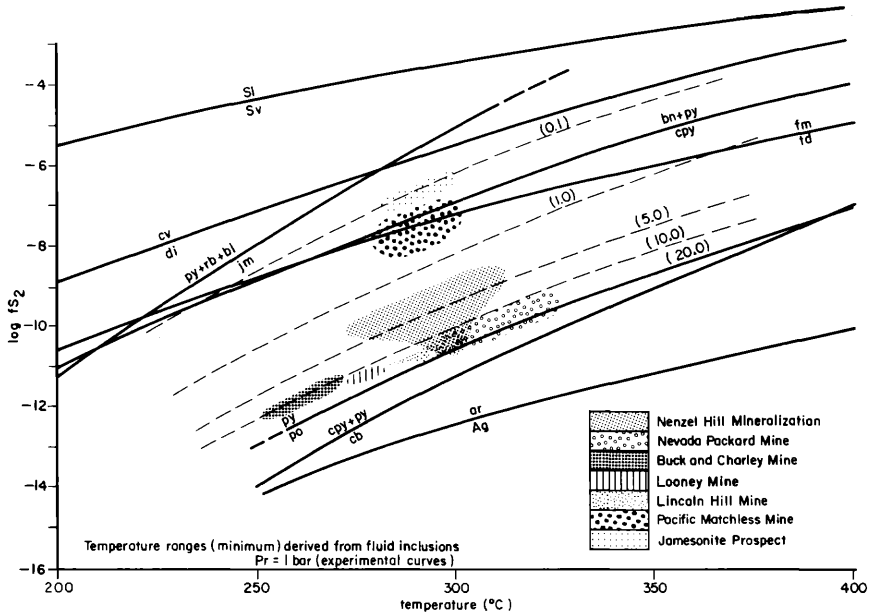

FIG. 17. Sulfur fugacity-temperature diagram relating the composition of sphalerite in mole percent FeS (numbered, dashed lines) to other univariant equilibria pertinent to sulfide assemblages in the Rochester district. The 20.0 mole percent FeS curve corresponds to the pyrite/pyrrhotite boundary. Mineral assemblages, ranges of sphalerite compositions, and temperature for selected deposits are patterned and the presence of pyrrhotite indicated. The Jamesonite prospect "field" is approximate, as no fluid inclusion temperature data exist. For discussion of individual deposits and data on sphalerite compositions refer to Vikre (1977). Sulfidation curves are from Czamanske (1974), Craig and Barton (1973), and Barton and Skinner (1979). Location of deposits is given in Figure 2.

ference in temperature and pressure among the forming veins and the vast volumes of rhyolite between the veins.

Ore fluid density

An approximate calculation based on the computed weight and measured volume of components of uniform fluid inclusions—80 volume percent of 6 weight percent NaCl solution and 20 volume percent liquid carbon dioxide, at 1 kb and 300°C—gives an ore fluid density of about 0.79 g/cm^3. This calculation assumes that the fluid inclusion (hydrothermal) phases are largely immiscible at 23°C (Takenouchi and Kennedy, 1964, 1965), the temperature at which the volumes of phases were measured. Comparison with fluids from some other precious metal and polymetallic vein deposits (Nash, 1972; Nash and Cunningham, 1973) suggests that Rochester district veins formed from fluids of similar salinity and density.

Ore fluid chemistry

Fugacity-temperature (Fig. 17) and isothermal fugacity-pH (Fig. 18) diagrams were assembled with reference to mineralization in the Rochester district. Figure 17 shows some sulfidation reactions among the species present in the Nenzel Hill silver deposits and other precious metal mineralization. It presents critical relations from which parts of Figure 18 were constructed. Figure 18 is calculated for 1 kb and 300°C, the approximate pressure and temperature of mineralization derived previously. The same plot at 450°C, near the maximum vein temperatures allowed by sulfosalt stabilities, shows only minor variations in field configurations.

Mineral stabilities, the molecular proportion of FeS in sphalerites, and hydrogen ion concentrations approximated from alteration assemblages and fluid inclusion analysis fix the range of sulfur and oxygen fugacities fairly definitively for Nenzel Hill mineralization (Fig. 18). The absence of hypogene iron oxides greatly reduces the range of possible depositional environments. Sphalerite compositions and the presence of chalcopyrite + pyrite rather than bornite + pyrite and tetrahedrite rather than famatinite restrict the upper sulfur fugacity to about 10^{-7} bars. The FeS content of sphalerites theoretically does not permit the existence of bornite and other hypogene copper sulfides at Nenzel Hill.

The presence of pyrrhotite, as well as sphalerite compositions, defines the lower range of sulfur fugacity. Initial f_{S_2} values in the hydrothermal fluid were less than $10^{-10.6}$ bars. Anglesite, graphite, and hematite do not occur in hypogene mineralization throughout the district and, thus, limit the range in

oxygen fugacity from about 10^{-37} to 10^{-30} atm. At measured f_{CO_2} the absence of both calcite and siderite in veins and wall rocks further restricts f_{O_2} to less than about 10^{-31} atm.

Carbon dioxide was an abundant constituent of hydrothermal fluids throughout the district, but no carbonate gangue minerals have formed in any of the precious metal veins. No evidence exists, such as silica pseudomorphs, which might suggest the former presence of calcite or siderite.

Stratigraphic reconstruction strongly indicates that an extensive thickness of Star Peak carbonate rocks covered Koipato rhyolites of Nenzel Hill prior to mineralization. At the Relief and Sheba mines (Ransome, 1909; Schrader, 1914; Cameron, 1939), nearby in the Humboldt Range, silver deposits were distributed laterally in limestones at the rhyolite contact. If the hydrothermal system was vertically confined just above the Star Peak-Koipato interface, lateral migration of ore solution in the carbonate section over Nenzel Hill may have enhanced circulation in underlying brecciated rhyolites. This would intuitively explain the abundance of carbon dioxide in vein fluid inclusions, but the absence of carbonate gangue associated with the mineralization is puzzling.

Calculations based on the data of Ellis (1959, 1963) and Ellis and Golding (1963) show that the pH-dependent calcite solubility curve for Nenzel Hill ore fluid lies at very high f_{O_2} and f_{S_2} values (Fig. 18). Calcite should be stable in the Nenzel Hill hydrothermal asemblage. The relatively high abundance of (Ca^{+2}) in hydrothermal solution ($\sim 10^{-1.1}$ according to fluid inclusion analyses) did not cause calcite precipitation, despite high carbon dioxide molalities, possibly because the solubility of $CaCO_3$ is essentially independent of $f_{CO_2} > 1$ bar at 300°C. Lack of evidence for boiling or carbon dioxide exsolution in the ore fluid, which might indicate a decrease in temperature and/or pressure, suggests that a homogeneous solution existed throughout mineralization. Because of high temperature and pressure, and possibly low pH, calcium carbonate remained in solution.

Siderite is not present in the hydrothermal assemblages because of high f_{S_2} and f_{O_2}, relative to f_{CO_2}, in the ore fluid (Fig. 18). In the Nenzel Hill ore-forming environment, siderite would be stable only with pyrrhotite and magnetite, according to the data of French (1971).

The pH-dependent activities of K^+ in equilibrium with sericite and kaolinite, and in equilibrium with sericite and K-feldspar in 1 kb (Montoya and Hemley, 1975; Usdowski and Barnes, 1972), define a stability field for sericite at values of $[K^+]$ reasonably consistent with fluid inclusion potassium concentrations for vein deposits (Roedder, 1972; Kamilli, 1976; Slack, 1976). Leachate analyses of the saline component of Nenzel Hill fluid inclusions indicate that the solute contains approximately $10^{-2.22}$ molal potassium, in good comparison with the K-feldspar-sericite equilibrium determined at 300°C and 1 kb by Usdowski and Barnes (1972).

Progressive increases in f_{S_2} and f_{O_2}, and a decrease in pH (at constant temperature and pressure) of the ore solution at Nenzel Hill, are indicated when vein mineral species, compositions, and textures are correlated with calculated sulfide and silicate mineral stabilities (Fig. 18). Vein sulfide assemblages characteristically change from iron-rich sphalerite + pyrrhotite + base metal sulfides to iron-poor sphalerite + silver sulfosalts with increasing elevation and, to a degree, stratigraphic level. Vein silicate assemblages also change from quartz + K-feldspar to quartz + sericite with elevation (Figs. 5, 9, and 10; Table 4).

The bulk of mineralization in the Nenzel Hill silver deposits formed in rhyolites that contained unaltered as well as partly sericitized orthoclase and microcline prior to mineralization. The initial sulfide phases, pyrrhotite, pyrite, iron-rich sphalerite, and tetrahedrite, probably precipitated from alkaline solutions (pH > 8) which did not metasomatize remaining wall-rock K-feldspar. The pH of ore fluids then decreased about one unit as most of the sulfides and silver sulfosalts were deposited within the sericite stability field, or at the K-feldspar-sericite boundary.

Discussion

The silver mineralization at Nenzel Hill compares in some respects but differs considerably from other precious metal vein districts in the western Great Basin, such as Tonopah, Virginia City, and Goldfield. Although quite diverse in detail, these famous silver-gold districts as a group share a number of significant characteristics:

1. They occur largely in extrusive and near-surface Miocene volcanic rocks.
2. Alteration and mineralization took place during volcanism, in part, or within 1 to 2 million years after the final eruptive event (Silberman et al., 1976, 1979).
3. The districts each produced more than one million ounces of gold and up to 200 million ounces of silver from ores that contained on the order of 0.5 oz Au and 10 oz Ag per ton (Bonham and Papke, 1969; Albers and Stewart, 1972; Bonham and Garside, 1974).
4. Stratigraphic reconstruction, vein textures, and hydrothermal assemblages suggest that the deposits formed at relatively low temperatures, primarily by open-space filling of fissures close to the paleosurface. Ore shoots in similar high-grade veins at Pachuca and Tayoltita, Mexico, were deposited at approximately 220° to 250°C at depths ranging from 1,200 to 1,500 ft (Dreier, 1976; Albinson, 1978).

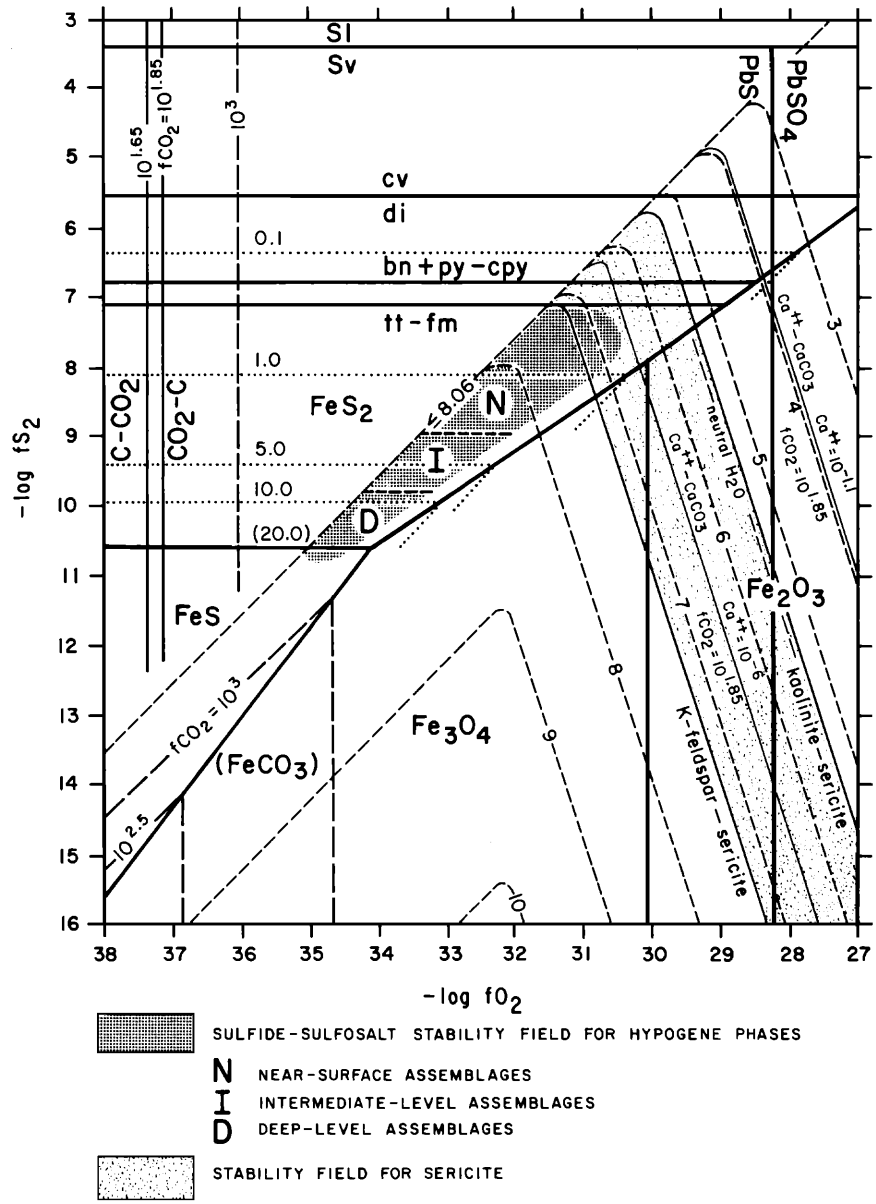

FIG. 18. Oxygen-sulfur fugacity-pH diagram compiled for the approximate environment of alteration-mineralization at Nenzel Hill, based on sulfide and silicate stabilities and compositions at elevated temperatures and pressures. Constraints: $\Sigma S = 10^{-1.0}m$, $(K^+) = 10^{-3.0}m$, T = 300°C, P = 1 kb, $f_{CO_2} = 10^{-1.65}$ (~13 volume percent CO_2), and $10^{-1.85}$ (~32 volume percent CO_2). Total sulfur used for pH calculations approximates that of some ore fluids (Ohmoto, 1972). The pH contours (thin, short dashed lines) are based on the stabilities of dissolved sulfur species at $\Sigma S = 10^{-1.0}m$. The boundary at pH-8.06 for the hypogene sulfide-sulfosalt stability field coincides with the upper limit for [ΣS] used in construction of the diagram. $(K^+) = 10^{-3.0}$ m is the lower value in the range 4,000 to 40 ppm which encompasses fluid inclusion concentrations from other vein-type hydrothermal deposits (Roedder, 1972). The positions of pH-dependent silicate stability fields (thin, sold lines) were derived from $(K^+) = 10^{-3.0}$ m, an approximate value for Nenzel Hill ore fluid, and experimental work (Usdowski and Barnes, 1972; Zen, 1972). The C/CO_2 and $Ca^{+2}/CaCO_3$ boundaries (thin, long dashed lines) were calculated at two f_{CO_2} values ($10^{-1.65}$; $10^{-1.85}$) near the compositional limits of the hydrothermal solution implied by fluid inclusion phase ratios. Hypothetical stability fields for siderite at $f_{CO_2} = 10^{3.0}$ and $f_{CO_2} = 10^{2.5}$ (thick, dashed lines) are included for reference. Thick solid lines mark stability fields for species in the system Fe-O-S. Dotted lines denote FeS contents of sphalerite. Dominant sulfur and carbon species in the hypogene sulfide-sulfosalt stability field are H_2S, HS^- and SO_4^{-2}, and H_2CO_3 and HCO_3^-, respectively. The position of near-surface, intermediate and deep level assemblages was derived from Figure 9 and Table 4. Limitations, assumptions, and sources of other data are given in Vikre (1977).

5. Based on stable isotope analyses, vein constituents precipitated mainly from meteoric water (O'Neil and Silberman, 1974).

The Rochester deposit occurs in eruptive volcanic rocks and easily ranks with Great Basin "bonanza" districts in total ounces of contained precious metals. Wall-rock alteration and some vein components at Rochester are also common to members of the Tertiary group. However, major differences are marked:

1. Mineralization at Nenzel Hill apparently took place more than 150 million years after Koipato volcanism.
2. Temperature and pressure at vein formation were on the order of 300°C and 1 kb, respectively. The estimated thickness of cover during mineralization at Rochester is considerably greater than that proposed for the Tertiary group.
3. Pyrite + pyrrhotite + high-iron sphalerite assemblages indicate a much lower f_{S_2}-f_{O_2} environment in Nenzel Hill veins than has been recognized in the Tertiary deposits.
4. The Rochester deposit is situated within a vast volume of rhyolite altered to quartz + sericite + pyrite ± K-feldspar. Between the numerous veins in Nenzel Hill this wall-rock assemblage is essentially identical to that comprising Koipato rhyolites throughout the district. Large volumes of hydrothermally altered volcanic rocks also occur in some Tertiary precious metal districts, but well-developed metasomatic selvedges of distinctive mineralogy usually flank veins. At Goldfield, for instance, gold-bearing ledges are enveloped by alunite-, kaolinite-, and montmorillonite-dominated assemblages which spatially relate to chemical changes in hydrothermal solution and indicate strong disequilibrium between ore fluid and wall rocks.

Chemical as well as physical gradients in deep vein hydrothermal systems, such as that which operated at Nenzel Hill, were probably quite small. Some Tertiary precious metal and base metal vein deposits that have formed near the surface show features such as telescoped zoning and clay alteration, indicative of rapid physical and chemical changes in ore solutions. It is unlikely that kaolinite-alunite alteration assemblages and high sulfidation states will develop in deep veins, as these assemblages may require the relatively high oxidation states of near-surface environments.

Evidence for hypogene deposition of minerals indicative of high sulfidation states toward the end of mineralization at Nenzel Hill is speculative at best. Evolution of the ore-forming environment can be reliably traced only to an assemblage characterized by quartz, sericite, K-feldspar, pyrite, tetrahedrite, and low iron sphalerite (Fig. 18). Because this assemblage occurs in major veins and large volumes of wall rock (Fig. 10), it may be assumed that the composition of the hydrothermal solution was relatively constant throughout Nenzel Hill during deposition of most silver mineralization. The common hypogene silicate minerals in both veins and low-grade mineralization suggest that the deposits were in mineralogical and chemical equilibrium with the enclosing wall rock.

Two potential buffers, dissolved carbonate species and quartz + sericite + K-feldspar, may be related to the pervasiveness of this assemblage. In a homogeneous hydrothermal fluid, the molarity of carbonic acid is reflected by the amount of dissolved CO_2 and significant amounts of HCO_3^- as well as H_2CO_3 were present in Nenzel Hill ore fluid. Calculations with high-temperature equilibria (Helgeson, 1969; Ryzhenko and Malinin, 1971) indicate that $[H_2CO_3] < [HCO_3^-]$ (300°C) at the pH suggested by the ubiquity of hydrothermal sericite in the Nenzel Hill vein system. At 300°C the $[CO_2]/[HCO_3^-]$ equilibrium pH is approximately 11 (Skinner and Barton, 1973). Although elevated pressure may promote the dissociation of H_2CO_3, the moderately high temperature during the vein mineralization largely excludes the possible control of pH by a CO_2-H_2O mixture. The H_2CO_3/HCO_3^- pair would respond directly to changes in $[H^+]$ rather than minimize the effects of slight increases or removal of hydrogen ion. At no time during the course of mineralization, then, were the hydrothermal fluids affected significantly by dissolved carbonate species.

The silicates K-feldspar and sericite were apparently far more successful in stabilizing the activities of critical dissolved species such as H^+ and K^+. Ore fluid was at least partially buffered by the quartz + sericite + K-feldspar assemblage which had developed in Weaver rocks prior to mineralization. Increasing $[H^+]$ was resisted by K-feldspar, while decreasing $[H^+]$ was negated by the presence of sericite according to the reaction:

$$1.5KAlSi_3O_8 + H^+ \rightleftarrows 0.5KAl_2AlSi_3O_{10}(OH)_2 + 3SiO_2 + K^+$$

and the Nenzel Hill hydrothermal system became solution controlled. Had the wall-rock rhyolites been an unaltered quartz + K-feldspar assemblage at the time of mineralization, well-developed quartz-sericite selvedges would probably flank the veins. It is doubtful that much low-grade mineralization would have formed as the sulfides would precipitate near major conduits in a zone of rapidly changing pH.

In addition to buffered wall rocks and low temperature-pressure gradients, the absence of mafic minerals in Koipato rhyolites allowed the Nenzel Hill ore fluid to circulate widely without appreciable changes in composition. Precious metal deposits in intermediate and mafic volcanic rocks with extensive alteration envelopes display strong disequilibrium between wall rocks and ore solutions. Calcium-iron-

magnesium minerals cause pH fluctuations through complex, largely irreversible reactions such as:

$$\underset{\text{anorthite}}{CaAl_2Si_2O_8} + 8H^+ \rightleftarrows Ca^{+2} + 2Al^{+3} + 2H_4SiO_4,$$

$$\underset{\text{biotite}}{KFe_3(AlSi_3O_{10})(OH)_2} + 10H^+ \rightleftarrows K^+ + 3Fe^{+2} + Al^{+3} + 3H_4SiO_4, \text{ and}$$

$$\underset{\text{hornblende}}{NaCa_2(Mg_2Fe_3)(Si_6Al_2)O_{22}(OH)_2} + 22H^+ \rightleftarrows Na^+ + 2Ca^{+2} + 3Fe^{+3} + 2Mg^{+2} + 2Al^{+3} + 6H_4SiO_4.$$

Sulfides in these deposits were rapidly precipitated in, and confined to, channel ways, with little distribution of vein constituents into wall rocks. In these cases hydrothermal solution chemistry was largely controlled by lithology.

Acknowledgments

This paper embodies part of the author's Ph.D. dissertation submitted to Stanford University. Appreciation is extended to ASARCO Incorporated for supporting post-thesis research, and to the U. S. Geological Survey for providing some of the K-Ar dates in Table 1. Careful reviews by F. T. Graybeal greatly enhanced graphic presentation of data and clarified numerous points.

April 22, November 6, 1980

REFERENCES

Albers, J. P., and Stewart, J. H., 1972, Geology and mineral deposits of Esmeralda County, Nevada: Nevada Bur. Mines Geology Bull. 83, 80 p.

Albinson, T., 1978, Fluid inclusion studies of the Tayoltita mine and related areas, Durango, Mexico: Unpub. M.S. thesis, Univ. Minnesota, 91 p.

Ashley, R. P., and Silberman, M. L., 1976, Direct dating of mineralization at Goldfield, Nevada, by potassium-argon and fission-track methods: ECON. GEOL., v. 71, p. 904–924.

Bailey, E. H., and Phoenix, D. A., 1944, Quicksilver deposits in Nevada: Univ. Nevada Bull., v. 38, no. 5, 206 p.

Barton, P. B., Jr., and Skinner, B. J., 1979, Sulfide mineral stabilities, *in* Barnes, H. L., ed., Geochemistry of hydrothermal ore deposits, 2nd ed: New York, John Wiley and Sons, p. 278–403.

Bonham, H. F., and Garside, L. J., 1974, Tonopah mining district and vicinity: Nevada Bur. Mines Geology Rept. 19, p. 42–46.

Bonham, H. F., and Papke, K. G., 1969, Geology and mineral deposits of Washoe and Storey Counties, Nevada: Nevada Bur. Mines Geology Bull. 70, 140 p.

Bonham, H. F., Garside, L. J., and Silberman, M. L., 1972, K-Ar ages of ore deposition at Tonopah, Nevada: Isochron/West, no. 4, p. 5–6.

Brown, P. E., Essene, E. J., and Kelly, W. C., 1978, Sphalerite geobarometry in the Balmat-Edwards district, New York: Am. Mineralogist, v. 63, p. 250–257.

Browne, P. R. L., and Lovering, J. F., 1973, Composition of sphalerites from the Broadlands Geothermal field and their significance to sphalerite geothermometry and geobarometry: ECON. GEOL., v. 68, p. 381–387.

Cameron, E. N., 1939, Geology and mineralization of the northeastern Humboldt Range, Nevada: Geol. Soc. America Bull., v. 50, p. 563–634.

Campbell, D. F., 1939, Geology of the Bonanza King mine, Humboldt Range, Pershing County, Nevada: ECON. GEOL., v. 34, p. 96–112.

Clynne, M. A., and Potter, R. W., 1977. Freezing point depression of synthetic brines [abs.]: Geol. Soc. America, Abstracts with Programs, v. 9, no. 7, p. 930.

Couch, B. F., and Carpenter, J. A., 1943, Nevada's metal and mineral production (1859–1940, inclusive): Nevada Bur. Mines Bull. v. 37, no. 4, p. 123–131.

Craig, J. R., And Barton, P. B., 1973, Thermochemical approximations for sulfosalts: ECON. GEOL., v. 68, p. 493–506.

Czamanske, G. K., 1974, The FeS content of sphalerite along the chalcopyrite-pyrite-bornite sulfur fugacity buffer: ECON. GEOL., v. 69, p. 1328–1334.

Dreier, J. E., 1976, The geochemical environment of ore deposition in the Pachuca-Real del Monte district, Hidalgo, Mexico: Unpub. Ph.D. dissertation, Univ. Arizona, 115 p.

Ellis, A. J., 1959, The solubility of calcite in carbon dioxide solutions: Am. Jour. Sci., v. 257, p. 354–365.

—— 1963, The solubility of calcite in sodium chloride solutions at high temperatures: Am. Jour. Sci., v. 261, p. 259–267.

Ellis, A. J., and Golding, R. M., 1963, The solubility of carbon dioxide above 100°C in water and in sodium chloride solutions: Am. Jour. Sci., v. 261, p. 47–60.

French, B. M., 1971, Stability relations of siderite ($FeCO_3$) in the system Fe-C-O: Am. Jour. Sci., v. 271, p. 37–78.

Garrels, R. M., and Christ, C. L., 1965, Solutions, minerals, and equilibria: San Francisco, Freeman, Cooper and Company, 450 p.

Hall, H. T., 1967, The pearcite and polybasite series: Am. Mineralogist, v. 52, p. 1311–1321.

Hanson, G. N., and Gast, P. W., 1967, Kinetic studies in contact metamorphic zones: Geochim. et Cosmochim. Acta, v. 31, p. 1119–1154.

Hart, S. R., 1964, The petrology and isotopic-mineral age relations of a contact zone in the Front Range, Colorado: Jour. Geology, v. 72, p. 493–505.

Jenney, C. P., 1935, Geology of the central Humboldt Range, Nevada: Univ. Nevada Bull., v. 29, no. 6, 73 p.

Johnson, M. G., 1977, Geology and mineral deposits of Pershing County, Nevada: Nevada Bur. Mines Geology Bull. 89, 115 p.

Kamilli, R., 1976, Paragenesis zoning, fluid inclusions and isotopic studies of the Finlandia vein, Colqui district, central Peru: Unpub. Ph.D. dissertation, Harvard Univ., 173 p.

Kelly, W. C., and Turneaure, F. S., 1970, Mineralogy, paragenesis and geothermometry of the tin and tungsten deposits of the eastern Andes, Bolivia: ECON. GEOL., v. 65, p. 609–680.

Kennedy, G. C., 1954, Pressure-volume-temperature relations in CO_2 at elevated temperatures and pressures: Am. Jour. Sci., v. 252, p. 225–241.

Kennedy, G. C., and Holser, W. T., 1966, Pressure-volume-temperature and phase relations of water and carbon dioxide, *in* Clark, S. P., ed., Handbook of physical constants: Geol. Soc. American Mem. 97, p. 371–383.

Kerr, P. F., 1938, Tungsten mineralization at Oreana, Nevada: ECON. GEOL., v. 33, p. 390–427.

—— 1940, A pinitized tuff of ceramic importance: Am. Ceramic Soc. Jour., v. 23, no. 3, p. 65–71.

Kerr, P. F., and Jenney, P., 1935, Dumortierite-andalusite mineralization at Oreana: ECON. GEOL., v. 30, p. 287–300.

Knopf, A., 1924, Geology and ore deposits of the Rochester district, Nevada: U. S. Geol. Survey Bull. 762, 78 p.

Kretschmar, U., and Scott, D. S., 1976, Phase relations involving arsenopyrite in the system Fe-As-S and their application: Canadian Mineralogist, v. 74, p. 364–386.

Kullerud, G., Yund, R. H., and Moh, G., 1966, Phase relations in the Fe-Ni-S, Cu-Fe-S, and Cu-Ni-S systems [abs.]: ECON. GEOL., v. 61, p. 804.

Lemmlein, G. G., and Klevtsov, P. V., 1961, Relations among the principle thermodynamic parameters in a part of the system H_2O-NaCl: Geochemistry, no. 2, p. 148–158.

McKee, E. H., and Burke, D. B., 1972, Fission-track age bearing on the Permian-Triassic boundary and time of the Sonoma orogeny in north-central Nevada: Geol. Soc. America Bull., v. 83, p. 1949–1952.

Montoya, J. W., and Hemley, J. J., 1975, Activity relations and stabilities in alkali feldspar and mica alteration reactions: ECON. GEOL., v. 70, p. 577–583.

Nash, J. T., 1972, Fluid inclusion studies of some gold deposits in Nevada: U. S. Geol. Survy Prof. Paper 800-C, p. C15–C19.

Nash, J. T., and Cunningham, C. C., 1973, Fluid inclusion studies of the fluorspar and gold deposits, Jamestown district, Colorado: ECON. GEOL., v. 68, p. 1247–1262.

Nolan, T. B., 1935, The underground geology of the Tonopah mining district, Nevada: Univ. Nevada Bull., v. 29, no. 5, 49 p.

Ohmoto, H., 1972, Systematics of sulfur and carbon isotopes in hydrothermal ore deposits: ECON. GEOL., v. 67, p. 551–578.

O'Neil, J. R., and Silberman, M. L., 1974, Stable isotope relations in epithermal Au-Ag deposits: ECON. GEOL., v. 69, p. 902–909.

Ransome, F. L., 1909, Notes on some mining districts in Humboldt County, Nevada: U. S. Geol. Survey Bull. 414, 75 p.

Robinson, B. W., and Ohmoto, H., 1973, Mineralogy, fluid inclusions, and stable isotopes of the Echo Bay U-Ni-Ag-Cu deposits, Northwest Territories, Canada: ECON. GEOL., v. 68, p. 635–656.

Roedder, E., 1967, Fluid inclusions as samples of ore fluids, *in* Barnes, H. L., ed., Geochemistry of hydrothermal ore deposits: New York, Holt, Rinehart, and Winston, p. 515–574.

—— 1972, Composition of fluid inclusions: U. S. Geol. Survey Prof. Paper 440-JJ, Chap. JJ, 164 p.

Rose, A. W., 1976, The effect of cuprous chloride complexes in the origin of red-bed copper and related deposits: ECON. GEOL., v. 71, p. 1036–1048.

Schmitt, H. H., ed., 1962, Equilibrium diagrams for minerals at low temperature and pressure: compiled and edited by the Geological Club of Harvard, Cambridge, Massachusetts, 199 p.

Schrader, F. C., 1914, The Rochester mining district, Nevada: U. S. Geol. Survey Bull. 580-M, p. 325–372.

Scott, S. D., 1973, Experimental calibration of the sphalerite geobarometer: ECON. GEOL., v. 68, p. 466–474.

Scott, S. D., and Barnes, H. L., 1971, Sphalerite geothermometry and geobarometry: ECON. GEOL., v. 66, p. 653–669.

Scott, S. D., and Kissin, S. A., 1973, Sphalerite composition in the Zn-Fe-S system below 300°C: ECON. GEOL., v. 68, p. 475–479.

Silberling, N. J., 1973, Geologic events during Permian-Triassic time along the Pacific margin of the United States, *in* Logan, A., and Hills, L. V., eds. The Permian and Triassic systems and their mutual boundary: Calgary, Alberta Soc. Petroleum Geologists, p. 345–362.

Silberling, N. J., and Wallace, R. E., 1967, Geologic map of the Imlay quadrangle, Pershing County, Nevada: U. S. Geol. Survey Map GQ-666.

—— 1969, Stratigraphy of the Star Peak Group (Triassic) and overlying lower Mesozoic rocks, Humboldt Range, Nevada: U. S. Geol. Survey Prof. Paper 592, 50 p.

Silberman, M. L., Chesterman, C. W., Kleinhampl, F. J., and Gray, C. H., Jr., 1972, K-Ar ages of volcanic rocks and gold-bearing quartz-adularia veins in the Bodie mining district, Mono County, California: ECON. GEOL., v. 67, p. 597–604.

Silberman, M. L., Johnson, M. G., Koski, R. A., and Roberts, R. J., 1973, K-Ar ages of mineral deposits at Wonder, Seven Troughs, Imlay, Ten Mile and Adelaide mining districts in central Nevada: Isochron/West, no. 8, p. 31–35.

Silberman, M. L., McKee, E. H., and Stewart, J. H., 1976, Igneous activity, tectonics, and hydrothermal precious metal mineralization in the Great Basin during Cenozoic time: Preprint, AIME Annual Meeting, Las Vegas, Nevada, 31 p.

Silberman, M. L., White, D. E., Keith, T. E. C., and Dockter, R. D., 1979, Duration of hydrothermal activity at Steamboat Springs, Nevada, from ages of spatially associated volcanic rocks: U. S. Geol. Survey Prof. Paper 458-D, 14 p.

Skinner, B. J., and Barton, P. B., 1973, Genesis of mineral deposits: Earth Planetary Sci. Ann. Review, v. 1, p. 183–211.

Slack, J. F., 1976, Hypogene zoning and multi-stage vein mineralization in the Lake City area, western San Juan Mountains, Colorado: Unpub. Ph.D. dissertation, Stanford Univ., 327 p.

Smith, D. M., Jr., 1978, The significance of silver-gold ratios at the Tayoltita mine, Durango, Mexico: Preprint, AIME Annual Meeting, Denver, Colorado, 1978, 4 p.

Smith, J. G., McKee, E. H., Tatlock, D. B., and Marvin, R. F., 1971, Mesozoic granitic rocks in northwestern Nevada: a link between the Sierra Nevada and Idaho batholiths: Geol. Soc. America Bull., v. 82, p. 2933–2944.

Takenouchi, S., and Kennedy, G. C., 1964, The binary system H_2O-CO_2 at high temperatures and pressures: Am. Jour. Sci., v. 262, p. 1055–1074.

—— 1965, The solubility of carbon dioxide in NaCl solutions at high temperatures and pressures: Am. Jour. Sci., v. 263, p. 445–454.

Tatlock, D. B., 1961, Redistribution of K, Na, and Al in some felsic rocks in Nevada and Sweden [abs.]: Mining Eng., v. 13, p. 1256.

Usdowski, H. E., and Barnes, H. L., 1972, Untersuchungen über das Gleichgewicht zwischen K-Feldspat, Quartz and Muscovit und die Anwendung auf Fragen der Gesteinsbildung bei tieferen Temperaturen, (K-feldspar-quartz-muscovite equilibrium and applications to low temperature rock-forming minerals) (abstract in English): Contr. Mineralogy Petrology, v. 36, p. 207–219.

Vanderburg, W. O., 1936, Reconnaissance of mining districts in Pershing County, Nevada: U. S. Bur. Mines Inf. Circ. 6902, 57 p.

Vikre, P. G., 1977, Geology and silver mineralization of the Rochester district, Pershing County, Nevada: Unpub. Ph.D dissertation, Stanford Univ., 404 p.

Vitaliano, C. J., 1944, Contact metamorphism at Rye Patch, Nevada: Geol. Soc. American Bull., v. 55, p. 921–950.

Wallace, R. E., and Silberling, N. J., 1965, Westward tectonic overriding during Mesozoic time in north-central Nevada: U. S. Geol. Survey Prof. Paper 501-C, p. C10–C13.

Wallace, R. D., Silberling, N. J., Irwin, W. P., and Tatlock, D. B., 1969a, Geologic map of the Buffalo Mountain quadrangle, Pershing and Churchill Counties, Nevada: U. S. Geol. Survey Map GQ-821.

Wallace, R. E., Tatlock, D. B., Silberling, N. J., and Irwin, W. P., 1969b, Geologic map of the Unionville quadrangle, Pershing County, Nevada: U. S. Geol. Survey Map GQ-820.

Willden, R., 1961, Major westward thrusting of post-middle Triassic age in northwestern Nevada: U. S. Geol. Survey Prof. Paper 424C, p. C116–C120.

Zen, E-an, 1972, Gibbs free energy, enthalpy and entropy of ten rock-forming minerals: calculations, discrepancies, implications: Am. Mineralogist, v. 57, p. 524–553.